TRIBHUVAN UNIVERSITY

INSTITUTE OF ENGINEERING

PULCHOWK CAMPUS

THESIS NO.: M-382-MSREE-2021-2023

Analysis of Solar Photovoltaic - Thermal System Using Simulation and Experimental Approach

by

Ashok Subedi

A THESIS

SUBMITTED TO THE DEPARTMENT OF MECHANICAL AND AEROSPACE ENGINEERING IN PARTIAL FULFILLMENT OF THE REQUIREMENTS FOR THE DEGREE OF MASTER OF SCIENCE IN RENEWABLE ENERGY ENGINEERING

DEPARTMENT OF MECHANICAL AND AEROSPACE ENGINEERING

LALITPUR, NEPAL

NOVEMBER, 2023

COPYRIGHT

TRIBHUVAN UNIVERSITY
INSTITUTE OF ENGINEERING
PULCHOWK CAMPUS

DEPARTMENT OF MECHANICAL AND AEROSPACE ENGINEERING

The undersigned certify that they have read, and recommended to the Institute of Engineering for acceptance, a thesis entitled **" Analysis of solar photovoltaic-thermal system using simulation and experimental approach"** submitted by Mr. Ashok Subedi (078MSREE004) in partial fulfilment of the requirements for the degree of Masters of Science in Renewable Energy Engineering.

Supervisor, Assoc. Prof. Dr. Hari Bahadur Darlami
Associate Professor
Department of Mechanical and Aerospace Engineering
IOE, Pulchowk Campus, TU

External Examiner, Er. Khem Bhandari
Alternative Energy Promotion Center
Kathmandu, Nepal

Tribhuvan University
Institute of Engineering
Department of Mechanical and Aerospace Engineering
Pulchowk Campus

Committee Chairperson, Dr. Sudip Bhattarai
Head of Department
Department of Mechanical and Aerospace Engineering
IOE, Pulchowk Campus, TU

Date: 2023-11-28

ACKNOWLEDGEMENT

The current study is the outcome of extensive collaboration and support from various individuals within the institute. I wish to express my sincere appreciation to Associate Prof. Dr. Hari Bahadur Darlami, who not only serve as the program coordinator of Renewable Energy Engineering at Pulchowk Campus but also acted as my thesis supervisor. He provided me with the opportunity, essential resources and invaluable guidance, offering insightful suggestions throughout the entire thesis project.

My gratitude also goes to Assistant Prof. Sanjaya Neupane for his continuous motivation and support throughout the thesis work. I am also grateful CES family, for generously providing the necessary equipment needed for the experiments.

I am thankful to EnergizeNepal for their academic support, which played a crucial role in enabling the successful completion of this thesis. Additionally, I am thankful to Mr. Krishna Prasad Timilsina, project monitoring and evaluation engineer at Institute for Solar Energy Research, Mr. Bikash Karki, renewable engineer and Mr. Sunil Khadka, PhD. candidate at University of Arizona for their valuable guidance and support throughout the thesis. I wish to acknowledge the contribution to all individuals who are directly or indirectly involved in this research project.

I am profoundly thankful to my parents for their unwavering emotional support during this challenging thesis journey. Lastly, but not least, I extend my appreciation to my colleagues, namely Anuj Poudel, Birendra Bhandari, Purushottam Khatiwada and Rajan Bhusal for their dedicated time and effort in assisting with my work.

ABSTRACT

One potential solution for overcoming the use of fossil fuels involves renewable sources like solar energy. The most efficient way of extracting the solar energy is through solar PV system which tends to decline as the temperature of cell rises. A promising approach to enhance both the electrical performance of PV and the acquisition of beneficial heat energy is through the implementation of photovoltaic-thermal (PVT) systems. This technology aims to increase overall system efficiency.

This research undertook the development and examination of a PVT water system employing a serpentine-type tube configuration. To analyse outlet and cell temperatures, ANSYS software was utilized. The investigation encompassed a range of mass flow rates, spanning from 0.001 kg/sec to 0.005 kg/sec, and three heat flux rates (600, 800, and 1000 W/m^2). The study also encompassed real-world testing under Nepal's weather conditions, following the parameters set in the simulation. Computational fluid dynamics (CFD) results unveiled peak thermal and electrical efficiencies of the system at 59.3% and 11.6%, respectively. Experimental testing yielded slightly lower figures, with thermal and electrical efficiencies measuring 53.5% and 10.4%, correspondingly.

Notably, the PV system's electrical efficiency was gauged at 9.6%, while the PVT system reached 10.4%, underscoring the PVT system's enhanced efficiency due to its cooling impact and lower cell temperatures compared to standalone PV systems. The study highlighted that thermal efficiency exhibited a direct correlation with mass flow rate, whereas cell temperature exhibited an inverse relationship with increasing mass flow rates.

TABLE OF CONTENTS

LIST OF TABLES

LIST OF FIGURES

LIST OF SYMBOLS

A	Area (m^2)
C_P	Specific Heat Capacity (J/KgK)
FF	Fill Factor (-)
F_R	Heat Removal Factor (-)
G	Global Irradiation (W/m^2)
I_m	Maximum Current (A)
V_m	Maximum Voltage (V)
V_{oc}	Open Circuit Voltage (V)
I_{sc}	Short Circuit Current (A)
Q_{abs}	Incident Energy after absorptance and transmittance (J)
Q_{in}	Incident Energy (J)
Q_{out}	Outgoing or Lost Energy (J)
Q_{use}	Useful energy (J)
T_{amb}	Ambient Temperature (^oC)
T_{cell}	Cell Temperature ($^oC/K$)
T_{in}	Fluid Inlet Temperature (^oC)
T_{out}	Fluid Outlet Temperature (^oC)
T_{ref}	Reference Temperature (^oC)
U_L	Overall Heat Transfer Coefficient (W/m^2K)
F_RU_L	Effective Heat Transfer Coefficient (-)
$F_R(\tau\alpha)_{eff}$	Optical Efficiency (%)
$\Delta T/G$	Heat Removal Parameters (m^2K/W)
β	Temperature Coefficient (%/K)
η_{Power}	Electrical Power Generation Efficiency (%)

η_{th}	Thermal Efficiency (%)
η_{el}	Electrical Efficiency (%)
η_{o}	Overall Efficiency (%)
η_{ref}	Reference Efficiency (%)
$(\tau\alpha)_{eff}$	Effective Transmittance-Absorptance (-)
F_R	Heat Transfer Correction Factor (-)
E_f	Primary Energy Saving Efficiency (%)
mi_w	Mass Flow Rate (kg/sec)

LIST OF ABBREVIATIONS

3D	Three Dimensional
AM	Air Mass
CFD	Computational Fluid Dynamics
DC	Direct Current
a-Si	Amorphous Silicon
Mc-Si	Monocrystalline Silicon
CO_2	Carbon Dioxide
CAD	Computer Aided Design
GHG	Greenhouse Gas
Sc-Si	Single Crystal Silicon
Pc-Si	Polycrystalline Silicon
PVT	Photovoltaic-Thermal
STC	Standard Test Conditions
LCOE	Levelized Cost of Electricity
TRNSYS	Transient System Simulation Tool

CHAPTER ONE: INTRODUCTION

1.1 Background

The need for food and energy is rising along with the global population. The continued rise in energy demand, which is largely met by burning fossil fuels, has been a global worry in many ways. (IEA, 2021) estimates that 81% of the world's energy consumption is met by fossil fuels, but these sources also provide 89% of the world's CO_2 emissions and 70% of its greenhouse gas emissions, which are the primary contributors to global warming and climate change (IPCC, 2022).With the huge CO_2 and greenhouse gas (GHG) emissions from these sources, it's critical to investigate alternative energy sources including solar, hydro, biomass, and geothermal energy as a way to both meet demand for energy and dramatically cut emissions (Tyagi, 2021).

Everywhere on Earth can receive energy from solar, which is a plentiful carbon-free energy source. In fact, the 4.3×109 TJ of solar energy that reaches Earth's surface in a single day is more than enough to meet the planet's 4.1×109 TJ annual energy needs (Lewis & Nocera, 2006). Fundamentally, the two main types of energy obtained from the sun are electricity and heat. The greatest benefit of solar energy is that it can be used at any production scale, from small-scale homes to large-scale factories connecting to the grid or operated off-grid, using a variety of technologies including photovoltaic, CSPs, or integrating system with other forms of energy sources. The solar technologies also require very little maintenance because, unless tracking devices are added, they don't have any moving parts. With an average power loss of just 0.5% per year, the technology has a longer lifespan of over 20 years (Jordan & Kurtz, 2013). Most crucially, the levelized cost of energy (LCOE) averaged across the globe in 2021 was $0.048/kWh, a reduction of 88% in just the previous ten years (Renewable Power Generation Costs in 2021, 2022). Solar energy is expanding more than other renewable energy sources due to technological improvement, increased efficiency, and lower investment costs, and it can be projected that it will rule the market in the future decades (Jaeger, 2021).

1.2 Problem statement

Solar insolation varies by geography, which is the main obstacle to solar energy. Site characterization is crucial since it affects the total size and production of the plant because of the fluctuating irradiation's impact on power output. Another obstacle in the

PV market is the need for a specific design when installing PV and Thermal panels for household use. Laying fully dependent on orientation, tilt angle, and roof slope (taking into account the installation at roof), all of which vary from location to location. Space requirement is the other issue where the shade and poor orientation have an impact on the space limits as well (Allan, n.d.). Decreasing efficiency of solar is also the issue, which only convert 15% to 20% of incident solar energy into electricity while absorbing over 90% of it and losing the remainder as heat. Because of this, the solar industry needs fresh innovations to encourage the adoption of effective and affordable solutions to these problems.

Combining electrical and thermal energy would be a revolutionary strategy that might simultaneously have a wide range of applications and require less space. The hybrid photo voltaic thermal (PVT) modules could be the considerable solution because this cutting-edge technology can give three times as much energy as a PV system of equal size and around 1.1 times as much thermal energy as a thermal system of comparable scale. Although having lower electrical and thermal efficiency than individual PV and thermal systems, the PVT system offers a higher efficiency usage of space covered. The other benefit is an extension of system lifespan since the heat is optimally utilized and the fluid that passes past the panel lessens thermal stress on the PV panel. Given all these benefits, PVT installations can be the most beneficial solutions for household hot water and electric space heating. In the context of Nepal this technology could be used for fulfilling electricity shortage and daily hot water mainly in the Himalayas and remote areas where there is no connection of the grid line. Further this technology could be used in the commercial as well as domestic buildings for space heating which could be the best alternative. This is the main reason behind conducting this study.

1.3 Objective

The main objective of this study is to analyse the performance of the solar photovoltaic-thermal system in the context of Nepal using simulation and experimental approach.

The specific objectives of this study are;

- To develop the 3D model and determine the outlet temperature of the water and cell temperature of solar PV based on the different mass-flow rate and heat flux using CFD approach
- To construct the solar photovoltaic-thermal system and test its performance
- To compare the simulation and experimental results

CHAPTER TWO: LITERATURE REVIEW

2.1 Photovoltaic-thermal system's working principle

As comparison to a PV and thermal system running separately, a PVT hybrid system integrates PV and thermal energy to deliver both electrical and thermal power with a better energy yield per unit area and, therefore, improved overall efficiency. The primary benefit of a hybrid PV/T system is its ability to concurrently supply electrical and hot water (also the space heating if the fluid used is air or gas) demands while only requiring a single location and one energy source. These systems typically consist of PV cells and a heat exchanger contained in an insulated casing, with the heat exchanger transferring the surplus thermal energy from the panel to a fluid that can then be pumped for various purposes, such as daily hot water, heating of space and pool, and so forth.

A hybrid PVT system's photovoltaic panels are made of semiconductor material, which absorbs sunlight and produces power from it. Direct current (DC) power is produced when sunlight strikes semiconductor material generating the electrons that are then caught by PV cells. In a hybrid PVT system, the thermal collector is often a flat plate or a group of tubes covered in a highly absorbent substance. Sunlight that is not collected by the solar cells is taken up by the thermal collector and transformed into heat. The heat is subsequently used to produce steam or hot water, depending on the system's particular design. So, this system may be suitable for homes with limited space and that require both electrical and thermal load; nevertheless, they are more expensive and still in the development stage, with very few installations globally compared to PV and thermal systems.

When compared to PV modules, PVT collectors are often twice as expensive or even three times as expensive, especially those with good heat removal quality. Using low-tech setups and materials has been proven to lower the cost to benefit ratio, but will result in poorer thermal performance because of design simplifications (Zondag et al., 2003).

2.2 Photovoltaic-thermal system development

In order to increase performance of PV and use the power and heat from the hybrid system, Martin Wolf presented the idea of PVT collectors for homes in the first study on the practicality of hybrid PVT systems in the 1970s (Wolf, 1976). Similar to this, Kern and Russell also conducted a system analysis on PVT and came to the conclusion

that these systems, depending on the applications and climatic conditions, could be excellent alternatives to individual PV and thermal systems and are more favourable for residential buildings with high heating requirements (Kern & Russell, 1978). Although while this study and others helped provide the groundwork for future research on PVT systems, most investigations conducted prior to 2000 were somewhat basic (Islam et al., 2016).

The performance of a hybrid PVT solar water system was modelled and simulated by Kalogirou using TRNSYS, and the findings showed that the hybrid system could simultaneously satisfy over 49% of a DHW requirement while increasing the mean annual efficiency of the PV system from 2.8% to 7.7%. Efficiency rose by 31.7% on an annual basis overall (Kalogirou, 2001).

For analysing the dynamic functioning of PVT systems, Chow concluded that a dynamic model of a PVT water collector with a single glazing was preferable to steady state analysis. He also found that photovoltaic conversion efficiency can rise by 2% at lower temperatures and a mass flow rate of 0.01 kg/sec (Chow, 2003).

Kalogirou and Tripanagnostopoulos created and tested hybrid system of PV/T at the University of Patras using pc-Si and a-Si PV modules along with water heat extraction devices. According to the findings, pc-Si systems produce electricity more effectively than a-Si systems, but have lower thermal yields. The paper's conclusion acknowledged that hybrid units have a higher chance of success because overall energy production was much higher and emphasized the necessity for economic development for these systems before they could be widely used (Kalogirou & Tripanagnostopoulos, 2006a).

Assoa and his team introduced an innovative design for a photovoltaic/thermal (PV/T) collector by employing a two-dimensional mathematical model for a collector utilizing two fluids (air and water) and featuring a metal absorber. To assess the impact of various factors, such as the water mass flow rate, on the collector's thermal efficiency, they conducted a parametric analysis. The results indicated that, under specific conditions involving collector length and fluid mass flow rate, the thermal efficiency of the collector could potentially reach up to 80%. This study suggest that there is still potential for enhancing the cooling of PV cells based on these findings (Assoa et al., 2007).

Adnan Ibrahim and his team designed two distinct photovoltaic-thermal (PVT) systems, each dependent on the type of fluid employed. The first system utilizes water and is designed with a spiral flow absorber collector, while the second system uses air

and features a single-pass rectangular tunnel absorber collector. According to the study, the water-based collector had a combined efficiency of 64%, including an electrical efficiency of 11%, compared to the air-based collector's combined efficiency of 55%, including an electrical efficiency of 10% (Ibrahim et al., 2009).

Matsuka's research aimed to investigate whether liquid cooled BIPV-T collectors could replace BIPV modules, using simulations to analyse various climate scenarios. The results showed that in tropical climates, roof installations of BIPV-T collectors could yield 15-25% more energy compared to BIPV, while moderate climates showed an 8-15% increase. The thermal efficiency was ten times higher than electrical efficiency (Matuska, 2012).

Khelifa et al. conducted an ANSYS simulation of a hybrid PVT system that had a design similar to the one used in this study. They found that the back temperature of the PV cell decreased by 15-20% when water flowed through the channel (Khelifa et al., 2016).

Abdul-Ganiyu et al. conducted a study comparing the technical and economic feasibility of PVT and traditional PV modules in Ghana's climate. They found that when connected to batteries, the PVT system performed better than the PV system, with an LCOE of $0.33/kWh compared to $0.45/kWh for the PV system, making PVT the more favourable option for an average peak solar hour of 4.6 hours. However, without batteries, he found PV as more economical system compared to PVT system (Abdul-Ganiyu et al., 2021).

Arslan et al., designed, manufactured and tested the finned type air fluid photovoltaic-thermal collector where both experimental and numerical analysis were performed under various flow rates of mass. ANSYS was used for the numerical analysis for predicting the PV module surface temperature before conducting the experiment and under the similar meteorological conditions experiment was performed for 0.031087 kg/sec and 0.04553 kg/sec mass flow rates. The findings showed that the electrical efficiency was improved by 0.42%. Thermal and electrical efficiencies of PV/T collector for 0.031087 kg/sec flow rate were 37.10% and 13.56% and for 0.04553 kg/sec flow rates they were 49.5% and 13.98% respectively (Arslan et al., 2020).

Karunasena et al., developed the 10 different PV/T collector and conducted the simulation using ANSYS to find the best design which will cool the solar PV and based on the simulation result, solar PV/T collector that showed the best result was manufactured which provided the most cooling effect to conduct the experiment. They used two 100Watts solar PV one without cooling and other with cooling effect to

conduct the experiment. The finding from both numerical and experimental showed the improved efficiency of the system which was integrated with the cooling system on the back side of the panel. Further the electrical efficiency was improved by 2.5% with increase in electrical power generation by 28% compared to the solar PV alone without cooling (Karunasena et al., 2020).

In context of Nepal the average global horizontal irradiation (GHI) reaches up to 5.5 kWh/m^{2}day in northwest part of country while it is in the range of 4.4 to 4.9 kWh/m^{2}day in the southern part of the country. The specific solar PV electricity output capacity of the country lies between 1400 kWh/kW$_p$ and 1600 kWh/kW$_p$ (= average daily total between 3.8 and 4.4 kWh/kW$_p$) (Nepal Energy Sector Synopsis Report - 2022, 2022).

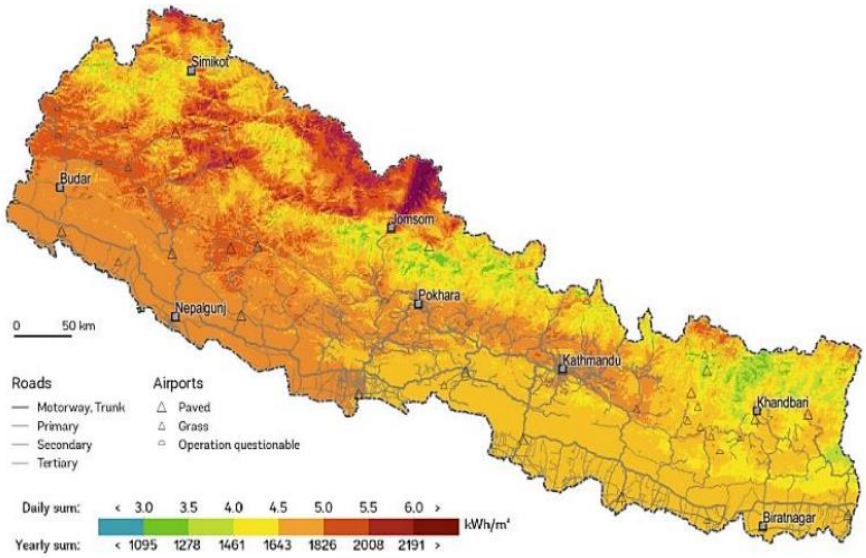

(Nepal Energy Sector Synopsis Report - 2022, 2022)

Figure 2.1: Global Horizontal Irradiation- a long-term average of daily and yearly total

Similarly, the maximum total solar radiation of about 777.27, 815.97, 914.03 and 704.51 W/m^2 were observed in Kathmandu, Pokhara, Lukla and Biratnagar respectively with annual average solar energy measuring 5.19, 5.44, 4.61 and 4.95 kWh/m^2/day for respective places (Poudyal et al., 2012). So, with this amount of generation of solar energy, it can fulfil the daily need which could be the best alternatives in the different parts of the country where there is no connection of the grid line. Further in the Himalayas region this could be used for fulfilling the daily hot water need to perform the daily activities and for space heating. Therefore, this technology could be useful and viable in context of our country.

It was noted that the performance of the solar photovoltaic thermal system is affected by different factors like thermal components and PV efficiency, system's design and configuration, operating conditions etc. Moreover, it can also be seen that this system has definite advantages over the individual systems. Thus, this study was focused on the CFD simulation of the serpentine type of collector and experiment was conducted on the same model of thermal collector to analyse the overall performance of the PVT system in context of Nepal. The results obtained from the simulation and experiment were compared with the result obtained from previous studies for the validation of the system.

CHAPTER THREE: METHODOLOGY

The research was all about the analysis of the solar photovoltaic-thermal system by two methods i.e., CFD simulation and experiment. The research procedure was segmented into four phases. Firstly, the literature review was conducted for finding the research gap and understanding the significant parameters that could adversely affects the performance of the solar PV device. Afterwards, 3D model of the solar PVT system was developed using the CAD software where the thermal collector was of serpentine type which was attached to the thermal absorber and enclosed by the insulation and framed together. Then the CFD simulation was conducted in ANSYS using mass flow rate and heat flux rate as the input parameters.

After conducting the simulation, the experiment setup was prepared and then experiment was conducted where the performance of the system was tested under the environmental conditions such as temperature, solar irradiation. The data collected from the experiment were analysed and compared with the simulation results. For the validation of the result obtained from the simulation and experiment, the results were compared with the previous research. Figure 3.1 shows the methodology that was adopted for conducting this study.

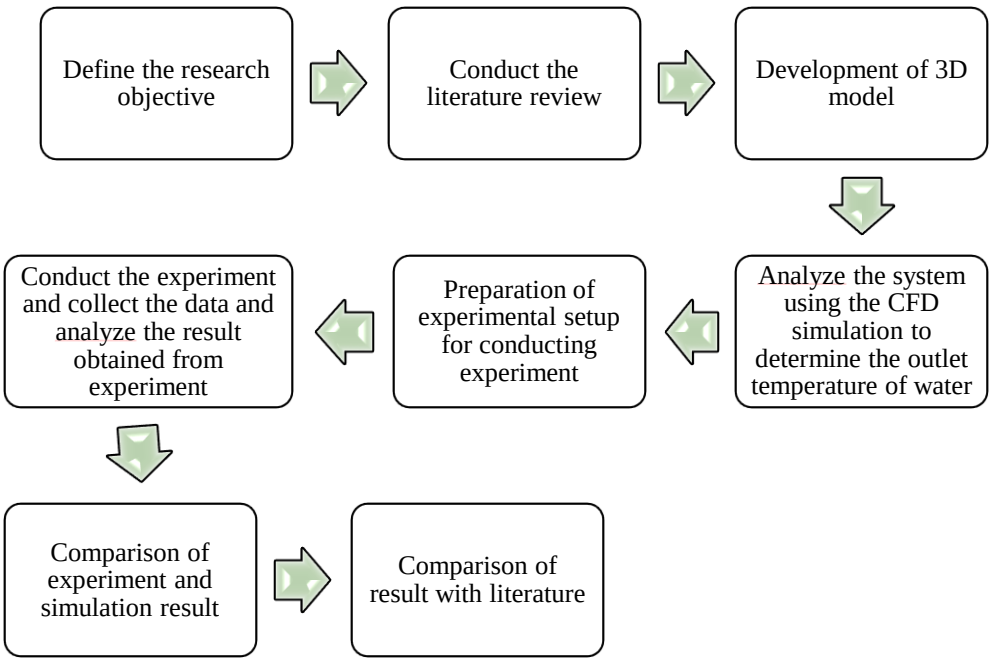

Figure 3.1: Flowchart showing the methods for conducting the research

3.1 Literature review

From the literature it was found that the performance of the solar photovoltaic thermal system is affected by different factors like thermal components and PV efficiency, system's design and configuration, operating conditions etc. Moreover it was also found that this system has definite advantages over the individual systems. Thus this study was focused on the CFD simulation of the serpentine type of collector and experiment was conducted on the same model of thermal collector to analyse the overall performance of the PVT system in context of Nepal. The results obtained from the simulation and experiment were compared with the result obtained from previous studies for the validation of the system.

3.2 Modelling and considerations

For designing and modelling literature review was conducted and based on the literature review, design consideration, assumptions and modelling was done which are explained in detail in following section.

3.2.1 Design consideration

The three-dimensional model of solar photovoltaic-thermal (PVT) system consists of glass, crystalline photovoltaic panel, thermal absorber and collector enclosed by the insulation layer and then framed together. Here in this study serpentine type of thermal collector was designed. Overall efficiency of the PVT system was affected by the various factors such as type of PV module, heat transfer fluid, glazing number, property of the thermal absorber and collector with mass flow rate of the fluid used in the system. The contact between the solar cell and thermal absorber was vital as the contact between these two components leads to the improvement of the efficiency. Here the water was chosen as the working fluid and copper as the material for the thermal components i.e., absorber and collector due to the superior properties of the copper compared to the other different materials like aluminum.

The designed 3D model has PV panel of size 450 mm × 340 mm with same size of thermal absorber plate. The thermal collector has 10 mm as the outer diameter and 9 mm as the inner diameter with 20 mm thickness of insulation. The design has 7 loops of pipes with 60 mm distance between each pipe. Figure 3.2 shows the different parts of solar PVT system developed using Solidwork software.

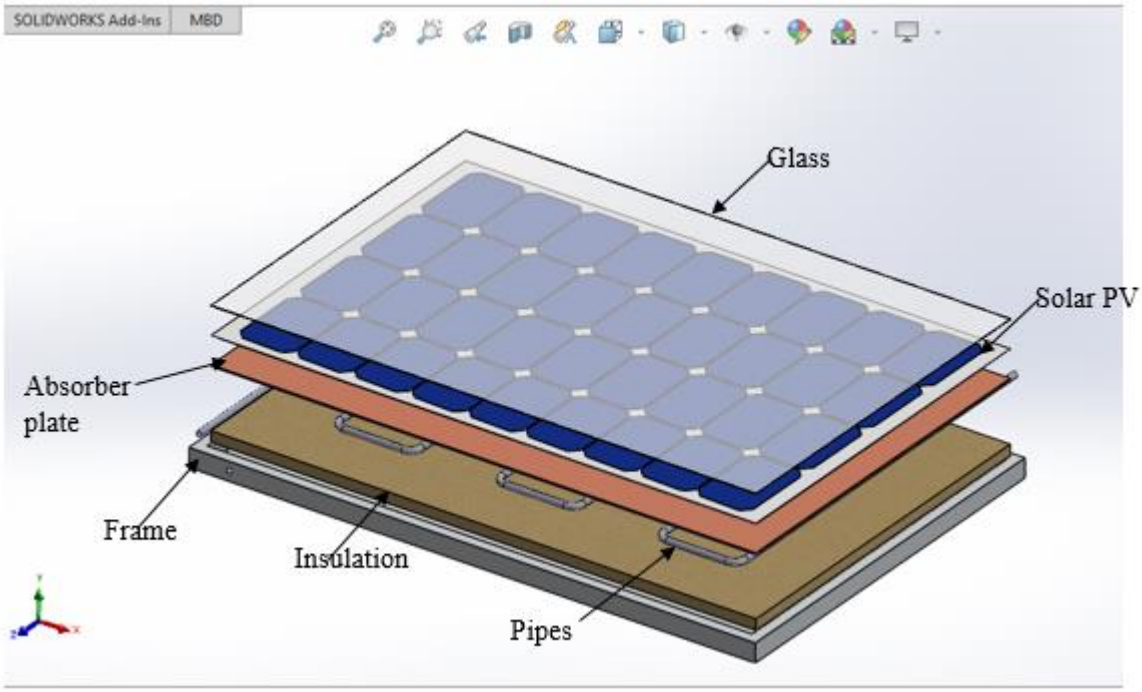

Figure 3.2: 3D model of solar photovoltaic-thermal system

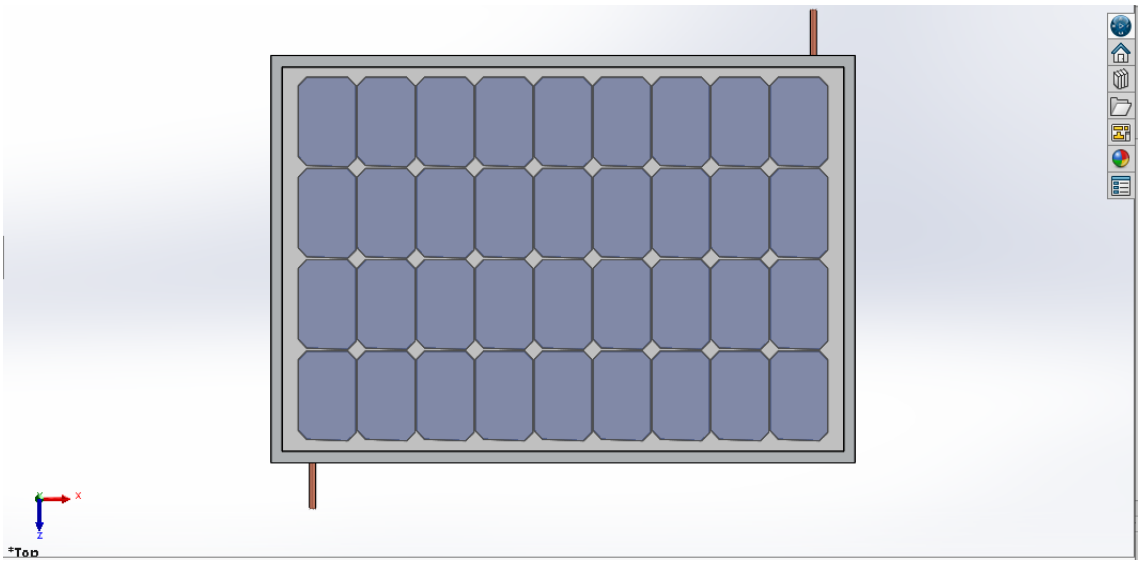

Figure 3.3: Top view of developed model

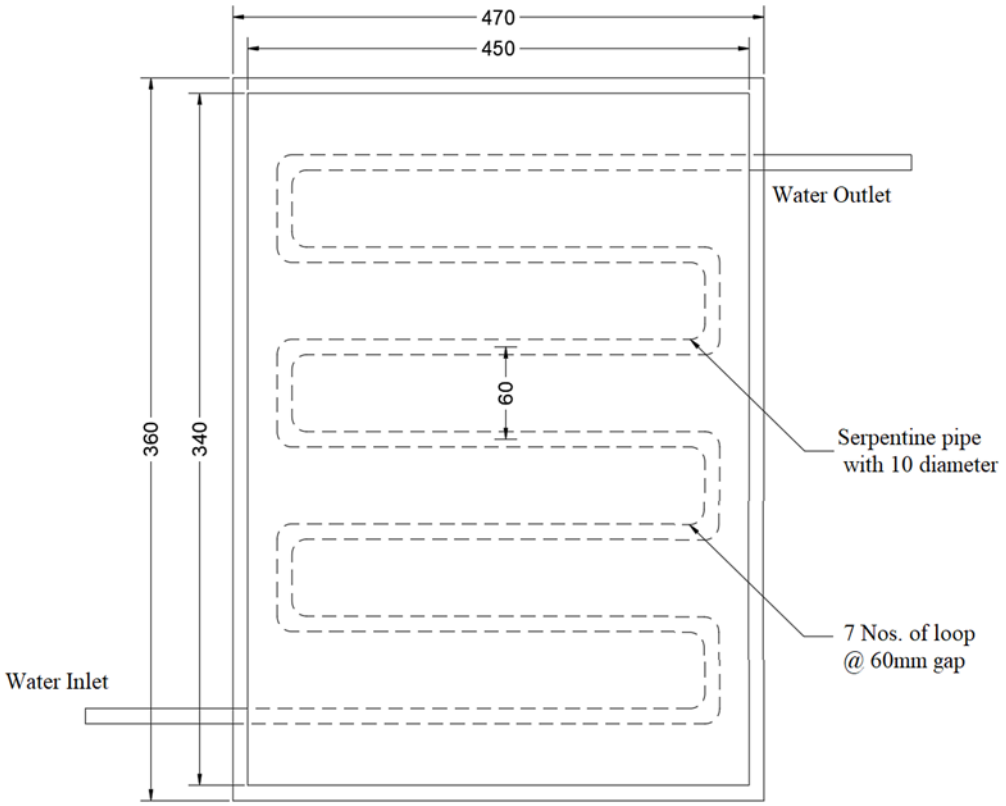

Figure 3.4: 2D Model (Top View)

Different materials are used for each part of the system which is tabulated in the Table 3.1;

Table 3.1: Material characteristics

S.N.	Parts	Parts thickness (mm)	Material	Density (kg/m^3)	Sp. heat capacity (J/kg.K)	Thermal conductivity (W/m.K)
1.	Glass	2	Glass	2200	480	1.1
2.	PV cell	1	Silicon	2330	700	148
3.	Plate	1	Copper	8960	385	401
4.	Pipes	-	Copper	8960	385	401
5.	Fluid	-	Water	998.2	4182	0.8
6.	Insulation	20	Rockwool	1.127	1000	0.03

Apart from this, different assumptions were considered while preparing the model which are as follow;

- Heat absorbed by the absorber plate was considered to be equivalent to the solar irradiation received by the PV module per square meter by neglecting the bonding between the PV module and absorber plate

- Transmittivity was assumed 100% considering that no air gap between the glass layer and PV module
- Unity packing factor was assumed i.e., the area of the PV module was equal to the area absorber plate
- Module was made or pure silicon so properties of silicon was used

3.3 Modelling

While conducting the modelling of the PVT system various assumptions were considered which are given below;

- The entire process operates in a steady-state condition
- Water was selected as the heat transfer fluid which also acts as coolant
- The ambient temperature remains consistent throughout the process and average temperature was taken into account for each layer
- Heat flux was irradiated constantly on the PV module
- Uniform water flows through the tubes and temperature gradient and pressure drop were neglected in the tubes
- Shading effect and losses from dust and dirt were neglected

Various parameters were calculated for determining the characteristics of the solar PVT system which are explained below with the necessary formula.

3.3.1 Electrical efficiency

PV module cell temperature are affected by the several factors and is the function of various variables like solar irradiation, speed of local wind, ambient temperature, system and material dependent properties like absorptance of plate, transmittance of glazing cover and so on. PV module electrical efficiency is significantly influenced by the module's cell temperature and can be expressed as the ratio of electrical power output to the incident solar radiation on the module which is given as;

$$\eta_{ele} = \frac{I_m \times V_m}{G \times A} = \text{Fill factor} \times \frac{I_{SC} \times V_{OC}}{G \times A} \tag{3.1}$$

where, V_m is the voltage and $I_m$is the current at maximum power conditions, I_{SC} and V_{OC} are short circuit current and open circuit voltage respectively. G and A are total solar irradiation and area of the PV module respectively. There is only slight

increase in short circuit current while fill factor and open circuit voltage both decreases with the temperature. Therefore, the net effect is linear equation which is as

$$\eta_{ele} = \eta_{Tref} + \beta(T_{out} - T_{ref}) \quad (3.2)$$

Where, η_{Tref} is the electrical efficiency of the PV module at the reference temperature (T_{ref}) and solar radiation of STC conditions i.e., 1000/m^2 at 25^0C with air mass ratio of 1.5, β is the coefficient of temperature of open circuit voltage which is normally given by the PV manufacturer and its values varies with the material and T_{out} is the outlet temperature.

In this study, all these specified values have been sourced from Luminous Polycrystalline solar panels where, η_{Tref} is 13.072%, β is -0.27%/K at STC conditions and T_{ref} is 25^0C.

3.3.2 Thermal efficiency

In a PVT system, thermal produces the thermal output while PV is in charge of the electrical output, and total efficiency is assessed as the sum of these two factors.

The total energy received by a PV module is usually converted into electrical and thermal energy to a certain extent, with some losses due to convection and radiation to lesser degree. The numerical model is constructed based on the equilibrium of these energy transfers both into and out of the system. Equation 3 provides the total solar energy from the sun that each module has captured (Duffie & Beckman, 2013)

$$Q_{in} = G \times A \quad (3.3)$$

Where, Q_{in} is the incident energy. The part of the Q_{in} is absorbed, transmitted and reflected therefore, the total incident energy after considering all the losses is given by equation 4;

$$Q_{abs} = ((\tau\alpha)_{eff}) \times G \times A \quad (3.4)$$

Where, $((\tau\alpha)_{eff})$= glazing's transmittivity and effective absorptivity.

Similarly, the formula for the energy lost is given as

$$Q_{lost} = U_L \times A \times (T_{cell} - T_{ambi}) \quad (3.5)$$

Where, U_L= coefficient of overall heat transfer, T_{cell} = average temperature of cell and T_{ambi}= ambient temperature.

Then the difference between total input energy and energy lost, which is determined by the cell's temperature and the overall heat transfer coefficient, is known as the total useful energy and given as;

$$Q_{use} = Q_{in} - Q_{lost} = ((\tau\alpha)_{eff}) \times G \times A - U_L \times A \times (T_{cell} - T_{ambi}) \quad (3.6)$$

As mentioned by (Duffie & Beckman, 2013), this equation 6 can be expressed in the form of Hottel-Whiller equation as given below;

$$Q_{use} = F_R \times A\left[\left((\tau\alpha)_{eff}\right) \times G\right) - U_L \times (T_{cell} - T_{ambi})\right] \quad (3.7)$$

Where, F_R is defined as the factor of heat removal which is the ratio of actual to the maximum possible heat transfer. As we know, the energy that is transferred to the working fluid from the collector and expressed as an increase in the temperature of the water leaving the absorber or collector is known as the total useful energy. This energy transfer is controlled by the rate of flow and the heat capacity of the water or flowing fluid and given as

$$Q_{use} = \dot{m}_w \times C_p \times (T_{in} - T_{out}) \quad (3.8)$$

Where, $\dot{m}_w$= water mass flow rate in kg/sec, C_p = water specific heat capacity in J/kgK and is taken as constant whose value is 4182 J/kgK, T_{in} and T_{out} are the inlet and outlet temperature of water respectively expressed in Kelvin.

As the above equation 8 governs the system's thermal energy so this can be used for calculating the system's thermal efficiency which is defined as the ratio of useful energy to the input energy. Therefore, thermal efficiency is given as;

$$\eta_{th} = \frac{Q_{use}}{Q_{in}} = \frac{\dot{m}_w * C_p * (T_{in} - T_{out})}{G * A} \quad (3.9)$$

3.3.3 Overall efficiency

Overall efficiency of PVT system is the sum of electrical and thermal efficiency which given as;

$$\eta_o = \eta_{ele} + \eta_{th} \quad (3.10)$$

The main energy used to generate the electricity should be taken into consideration when evaluating overall efficiency because the electricity is valued more due to its higher exergy, as in equation 3.2 (Schön, 2017).

3.4 CFD configurations

The one of the aim of this study is to simulate the designed model for generating the possible data to analyze the heat transfer and to observe the variation of the temperature in the fluid by changing the input parameters such as heat flux rate and mass flow-rate. To simulate and analyze the data, ANSYS fluid-flow (Fluent) 2021 R1 version was used and outlet temperature was analyzed by varying the mass flow rate and heat flux as input. Following assumptions were also made in addition to the assumption mentioned in the previous section;

- Incompressible work fluid
- PV cells absorbs all heat flux applied on top of the glass surface

3.4.1 ANSYS geometry and meshing

The 3D model prepared in Solidworks was saved in parasolid format and then imported in ANSYS geometry modeler where six sections were created in modeler namely glass, solar PV, absorber plate, collector pipe, fluid and insulation neglecting the enclosure in ANSYS.

After that meshing was performed which is the process of splitting the geometry into various nodes and elements for distributing the load uniformly i.e., heat flux rate in this study. Because of the geometry complexity, automatic meshing was used as it is faster than manual process of creating mesh. During the meshing different mesh element sizes ranging from 1mm to 4mm were used to create the fine mesh and to conduct the mesh independence test. It was found that when increasing the element size above 4mm there was no significant change in the result thus for the simulation 4mm of element size was used and analysis was conducted. For the generated mesh it was found that the average and maximum skewness were 0.1444 and 0.71269 respectively in less than 1 percent elements where nodes and elements numbers were 296920 and 212359 respectively.

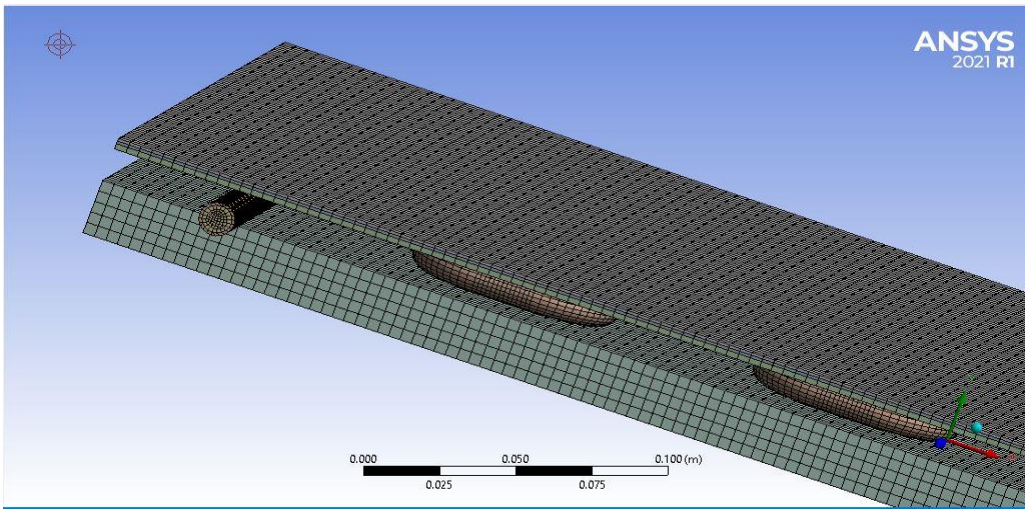

Figure 3.5: Meshing

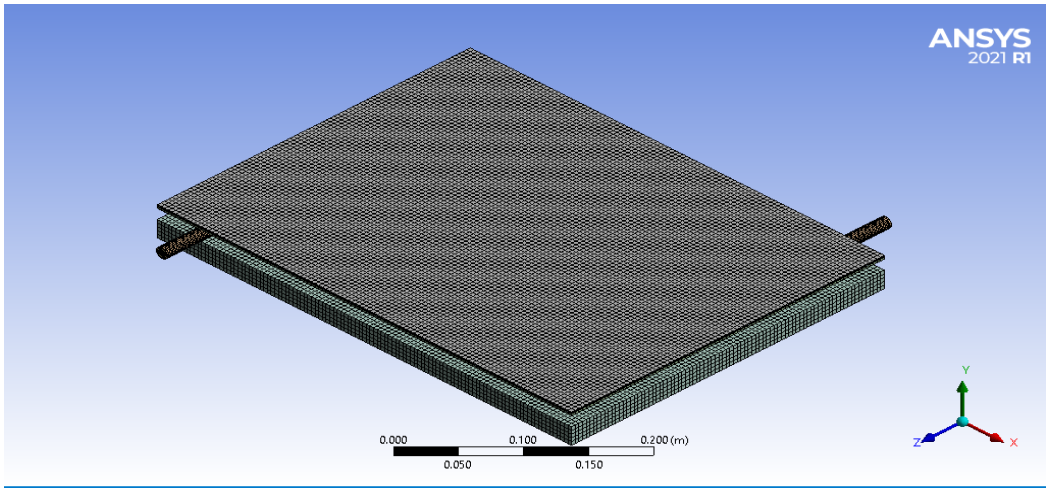

Figure 3.6: Isometric view of meshed model

3.4.2 Boundary conditions

Based on the literature review, governing equation and assumptions, boundary conditions were set. The boundary conditions that were used during the simulation were mention in the Table 3.2;

Table 3.2 : Boundary conditions

Description	Condition/values
Analysis type	Steady state
Reference pressure	1 atm
Material Characteristics	Refer Table 3.1
Condition of inlet	
Working fluid	Water
Heat Flux	Varying on glass top surface (600-1000 W/m^2)
Flow condition	Varying mass flow rate (ranges from 0.001 to 0.005 kg/sec)
Temperature of inlet	300K
Condition of outlet	Pressure outlet
Temperature of ambient	298.15K
Wall	No slip conditions

Weather conditions of Kathmandu was studied from the different sources and found that the maximum total solar radiation of Kathmandu was about 777.27 W/m^2 with annual average solar energy measuring 5.19 kWh/m^2/day. Therefore, while conducting the simulation 800W/m^2 was used and the result obtained from this will be compared with the result obtained from the experiment for validation purpose.

3.5 Experimental setup

Experimental setup was prepared for investigating the both thermal and electrical performance of the solar PVT water system with serpentine type pipe collector. The setup was constructed by using luminous polycrystalline solar PV of 20W. To prepare the PVT water system copper plate of thickness of 1mm was used as the thermal absorber which was brazed with the copper pipe having 10 mm and 9 mm as the outer and inner diameter respectively. The pipe was bend in such a way that it forms the serpentine type with 60 mm as the distance between each pipe. There were 7 loops of pipe. Below the pipe insulation of 20 mm thickness was used and all the components were frame together.

For circulating the water through the pipes, 15W DC pump was used which was attached to storage tank. To control the flow of the water manual valve was connected after the pump at the inlet side and the flow rate was measured by noting the time to fill the calibrated mug and volume of water collected per minute. To measure the inlet and outlet temperature of the water clamp meter was used by connecting the k-type thermocouple probe in the clamp meter. Similarly for measuring the current and voltage of the solar PV and PVT water system DT830D digital multimeter was used. The data obtained during the experiment was manually noted down by observing the reading

shown by the different instruments used during the experiment. For measuring the global irradiation manual pyranometer was used where the reading ranges from 0 to 1200 W/m^2. All the instrument that was used during the experiment has different uncertainty values. The experiment was carried out at Khashi Bazar, Kalanki, and Kathmandu for seven days. The specification of the Solar panel used for the experiment is given in the Table 3.3;

Table 3.3: Specification of Solar panel

Model No.	LUM020P
Serial No.	8121608
Production date	2016-08---
Peak power/P_{max} (W)	20
Power tolerance range (W)	0~+3
Open circuit voltage/ V_{oc}(V)	21.62
Rated voltage/V_{mp} (V)	17.70
Short circuit current / Isc (A)	1.21
Rated current/ I_{mp} (A)	1.13
Max. system voltage (V)	600
Dimension (mm)	450×340×18
Weight (kg)	1.8
Series fuse rating (A)	10

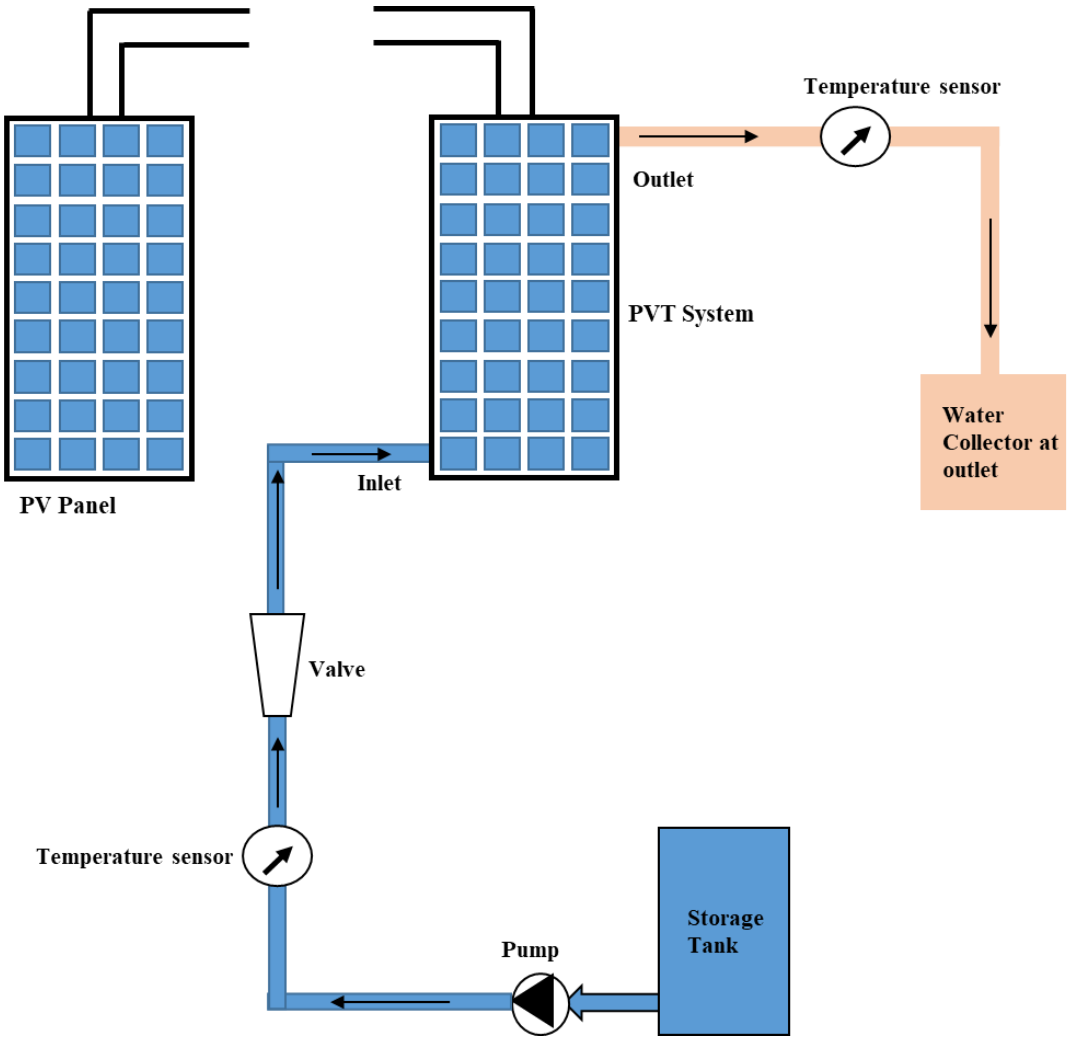

Figure 3.7: Schematic diagram of experiment

During the experiment, the mass flow-rate of the water was varied using the valve and the different parameters mentioned above were measured to determine the thermal and electrical performance of the solar PVT water system. After recording the parameters, the effect of the flow rate on the thermal and electrical efficiency of the solar PVT were studied and analyzed. Then the result obtained from the experiment was compared with the simulation result and with the literature for the validation of the study.

3.6 Comparison of the results

The result obtained from the CFD and experiment was compared for the validation of the study. Different parameters such thermal efficiency, electrical efficiency, overall efficiency, temperature difference was compared.

Further the results of the study were compared with the literature to validate the study. For this purpose, different research paper was used which were conducted previously by different approach. The detail comparison will be discussed in the following section.

CHAPTER FOUR: RESULTS AND DISCUSSION

Here in this section the result obtained from the simulation and experiment are presented. The results from ANSYS were obtained after running the solver by applying the necessary boundary condition such as various mass flow rate and different heat flux rate as input. Similarly, the experiment was conducted for seven days and the average value were taken for the calculation of the various parameters. Further the results obtained from the CFD were compared with the experiment and literature for the validation of the study.

4.1 Analysis of efficiencies using CFD

ANSYS 2021 R1 was used for simulation where mass flow rate and heat flux rate were taken as input parameters and water average outlet temperature flowing through tubes and average cell temperature were noted. In total 15 simulations were conducted for five different mass flow rates ranging from 0.001 kg/sec to 0.005 kg/sec with three different heat flux rate i.e., 600, 800 and 1000 W/m^2. The results obtained for different heat flux rate were explained below in details.

4.1.1 Thermal efficiency at 600 W/m^2

Thermal efficiency depends on the temperature difference between the inlet and outlet. In this study, the inlet temperature was maintained at 300K i.e., constant throughout the simulation while the outlet temperature of water passing through the collector was measured.

The temperature contour obtained from the simulation for 0.005 kg/sec mass flow rate is shown in the Figure 4.1;

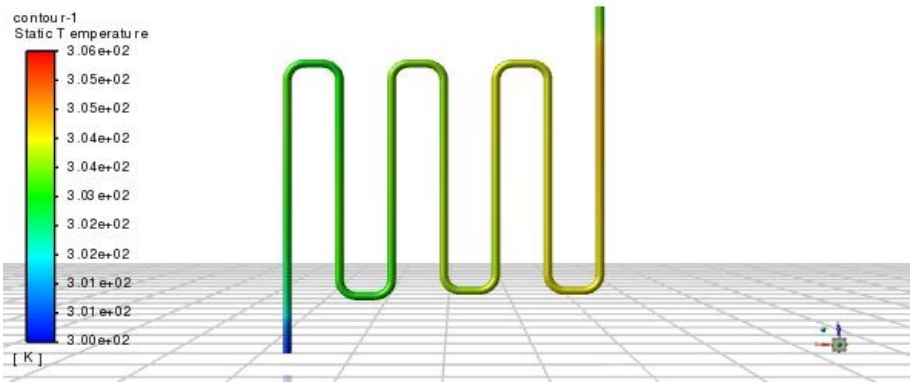

Figure 4.1: Static temperature contour for 0.005 kg/sec at 600 W/m^2

From the above temperature contour, it was observed that the inlet section has the lower temperature while outlet section has the higher temperature distribution. As the fluid passes through the thermal collector, the temperature of the flowing fluid i.e., water in this case start increasing by carrying out the heat generated in the system. Further, it can also be seen that the outlet section has slightly lower temperature compared to the other portion of the outlet section which is due to the loss of the heat to the surrounding as that part is not insulated during the simulation.

Figure 4.2 shows the fluctuation of the temperature difference and thermal efficiency at 600 W/m^2 heat flux.

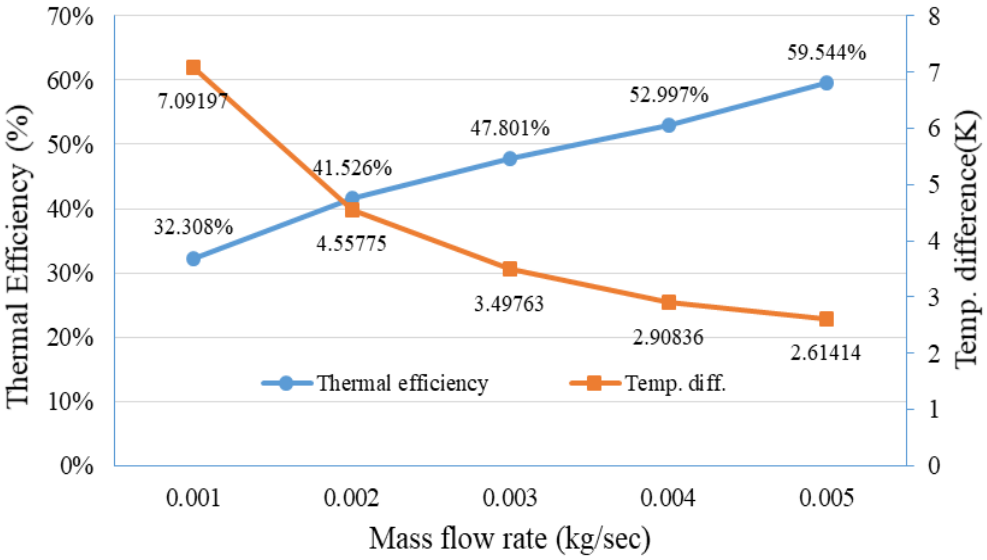

Figure 4.2: Variation of temperature difference and thermal efficiency at 600 W/m^2

The above Figure 4.2 shows, how the thermal efficiency and temperature difference between the inlet and outlet varies with the mass flow rate. It is clearly seen that the thermal efficiency is increasing while the temperature difference is decreasing with the increased mass flow rate. Thermal efficiency is maximum at 0.005 kg/sec of mass flow rate where the temperature difference is 2.614K. There is maximum increase in the thermal efficiency when the mass flow rate is change from 0.001 kg/sec to 0.002 kg/sec which is almost 28.53%. However, the overall increment of thermal efficiency is 84.30% when mass flow rate changes from 0.001 kg/sec to 0.005 kg/sec with decrease in temperature of just 4.478K. Therefore, based on the desired thermal efficiency and exit temperature the mass flow rate should be optimized.

4.1.2 Thermal efficiency at 800 W/m^2

The simulation was repeated by changing the heat flux rate for all the five different mass flow rates as explained in above section 4.1.1. The static temperature contour of serpentine pipe at 0.005 kg/sec flow for 800 W/m^2 heat flux is shown in the Figure 4.3 where the exit temperature of the flowing fluid was 303.472K.

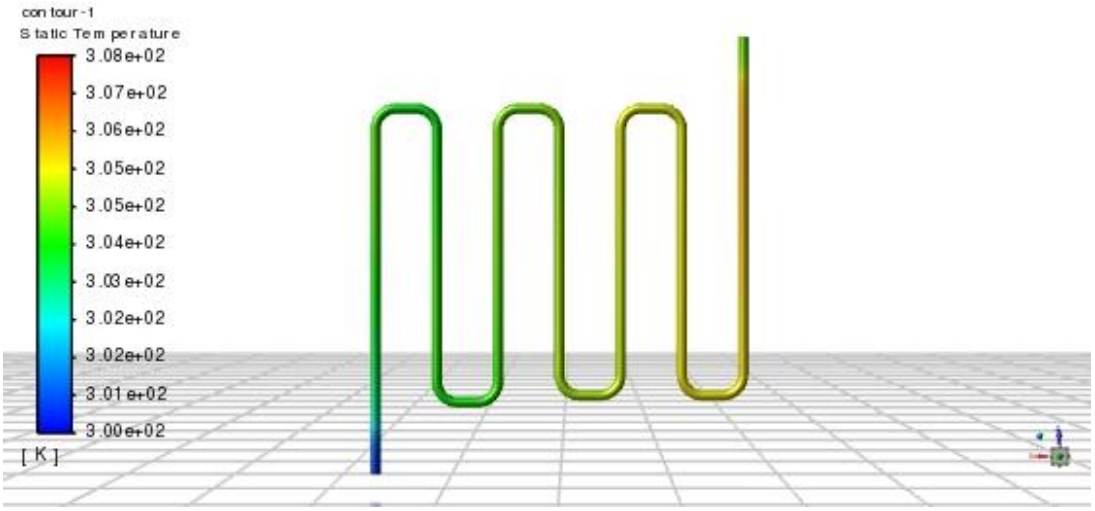

Figure 4.3: Static temperature contour for 0.005 kg/sec at 800 W/m^2

Figure 4.3 shows the distribution of the temperature of fluid in the pipe where it can be seen that the temperature is slightly increasing as it passes through the pipe from inlet to outlet section. The different color pattern shown in the figure indicates the temperature range and it increases by carrying the heat generated by the system. The inlet temperature was 300K and the outlet temperature reaches to 303.472K. From the figure it is clearly observed that the outlet section has slightly lower temperature compared to the other section of the outlet section as that part was exposed to surrounding and heat is lost to the surrounding. The global range of the temperature distribution vary from 300K to 308K which is shown in the color pattern in the left side of the figure.

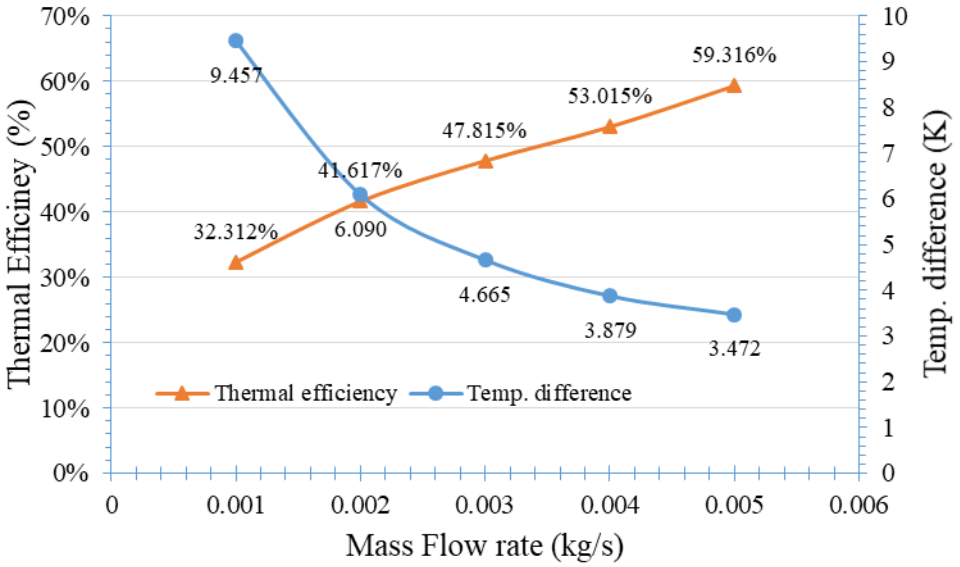

Figure 4.4: Variation of temperature difference and thermal efficiency at 800 W/m^2

Here Figure 4.4 shows the variation of the thermal efficiency and temperature difference between the outlet and inlet of water with the various mass flow rate. From the graph it can be seen that the as the mass flow rate increased then the thermal efficiency start increasing which is similar in tread with the previous section result. The result shows that the maximum change in the thermal efficiency was about 28.8% when the flow rate changes from 0.001 kg/sec to 0.002 kg/sec compared to other flow rates. Moreover, there was about 83% change in the thermal efficiency overall when the flow rate increases from 0.001 to 0.005 kg/sec for just temperature decrease of 5.985K. The following graph shows the relation between the mass flow rate, thermal efficiency and temperature difference.

4.1.3 Thermal efficiency at 1000 W/m^2

Figure 4.5 shows the distribution of temperature of the fluid throughout the pipe for 0.005 kg/sec flow rate at 1000 W/m^2 of heat flux.

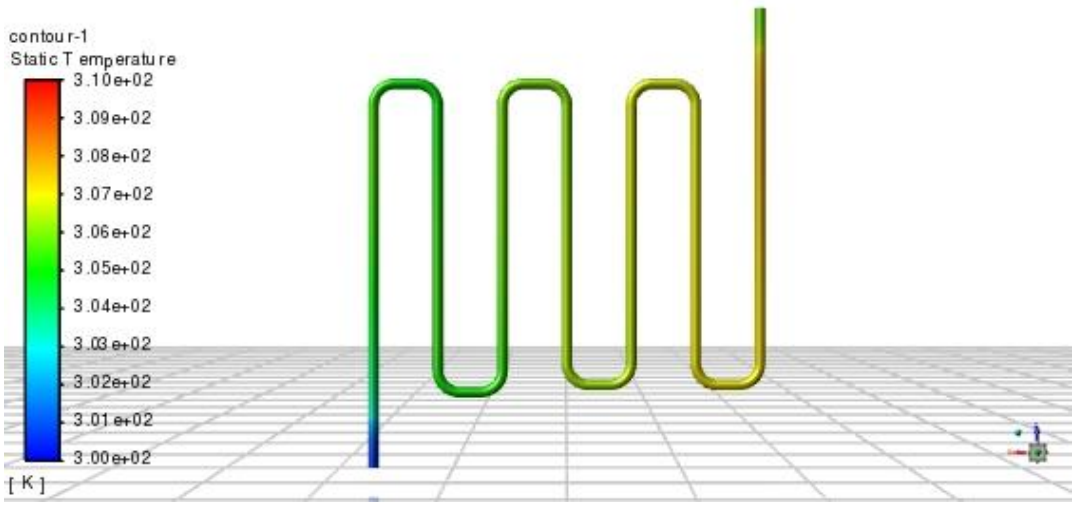

Figure 4.5: Static temperature contour for 0.005 kg/sec at 1000 W/m^2

Here, from Figure 4.5, it was analyzed that the temperature of the flowing fluid increases as it passes through the pipe which was under the solar panel as the flowing fluid took the heat generated thus increasing its temperature. The outlet temperature was 304.341K which was higher than inlet temperature by 4.341K. This provides the cooling effects to the panel and capture the thermal energy generated during the simulation. From figure, it was clearly observed that the pipe loops in the left side have the lower temperature compared to the pipe loops in the right side. This was due to the heat carried out by the fluid and the outlet portion of the pipe has lower temperature which is because of exposing the pipe to the surrounding.

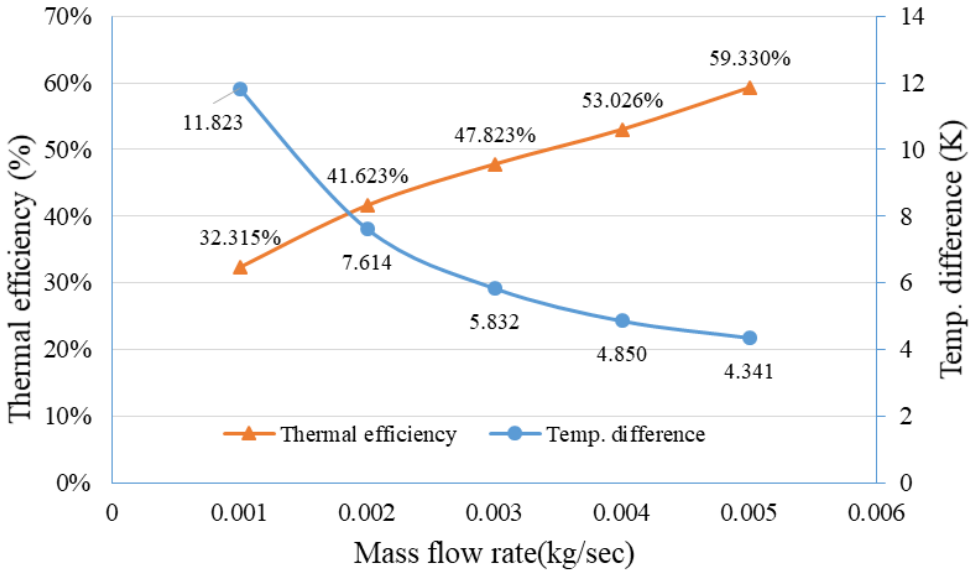

Figure 4.6: Variation of temperature difference and thermal efficiency at 1000 W/m^2

The result shows that the outlet temperature reaches to maximum value of 311.823K for the flow rate of 0.001 kg/sec with thermal efficiency of 32.315%. Here in this case also the change in the thermal efficiency was maximum when the flow rate increase from 0.001 to 0.002 kg/sec which was about 28.80%. On comparing the overall increment of the thermal efficiency, it is found that the thermal efficiency was increased by 83.6% for just decrease in the temperature of 7.482K. Further, the heat generated varies from 49 J/sec to 91 J/sec where the heat was maximum at the higher mass flow rate means heat dissipation rate was higher at the higher flow rate thus providing the better cooling effect at the higher flow rate as shown by the result above.

4.1.4 Variation in thermal efficiency

Thermal efficiency of the system varies for the different flow rate at different heat flux. The comparison of the thermal efficiency at various heat flux rate is shown in the Table 4.1.

Table 4.1: Comparison of thermal efficiency at various heat flux

ṁ (kg/sec)	Thermal efficiency, ηth (%)		
	G=600 W/m^2	G=800 W/m^2	G=1000 W/m^2
0.001	32.308%	32.312%	32.315%
0.002	41.526%	41.617%	41.623%
0.003	47.801%	47.815%	47.823%
0.004	52.997%	53.015%	53.026%
0.005	59.544%	59.279%	59.330%

Table 4.1 compares the thermal efficiency of the system at various input parameters assigned during the simulation. It was found that the thermal efficiency was almost similar in all the cases while there was slightly higher efficiency at higher heat flux compared to lower heat flux for lower flow rate. Further, it was also observed that the thermal efficiency increases with the mass flow rate irrespective of the heat flux rate. The central idea of the thermal system of PVT system was to provide the cooling effect for the PV panel and to generate the hot water but at the higher mass flow rate the difference in temperature between the inlet and outlet was very low which does not meet the hot water requirement. Despite, this the cooling can be effective with the higher flow rate as the more heat was dissipated with the higher flow rate.

On comparing the thermal efficiency obtained from this study with the results obtained by various researcher, it was found that the thermal efficiency aligns with the previous literature results. As per (Yang et al., 2018), the thermal efficiency was 58.35% which

shows that the thermal efficiency obtained from this study was nearly 1.6% higher thus validating the result obtained from the simulation. Similarly, when comparing the thermal efficiency of this study with study conducted by (Misha et al., 2020) shows that the thermal efficiency align with his study where it was only 0.5% less compared to (Misha et al., 2020) thus validating the result.

Further, as per (Herrando et al., 2019), the thermal efficiency vary from 65.55% to 67.45% which was nearly 13% higher than the thermal efficiency obtained from the simulation. Overall, when comparing with different literature, the thermal efficiency varies from 0.5% to 13% showing the similar trend thus validating the result obtained from the simulation.

4.1.5 Electrical efficiency

Electrical power is considered more valuable in solar PV compared to the thermal power and the electrical efficiency is determined based on the outlet temperature and temperature coefficient of open circuit voltage as mention in the earlier section. The temperature contour for different heat flux with 0.005 kg/sec mass flow rate are shown in the Figure 4.7 to Figure 4.9;

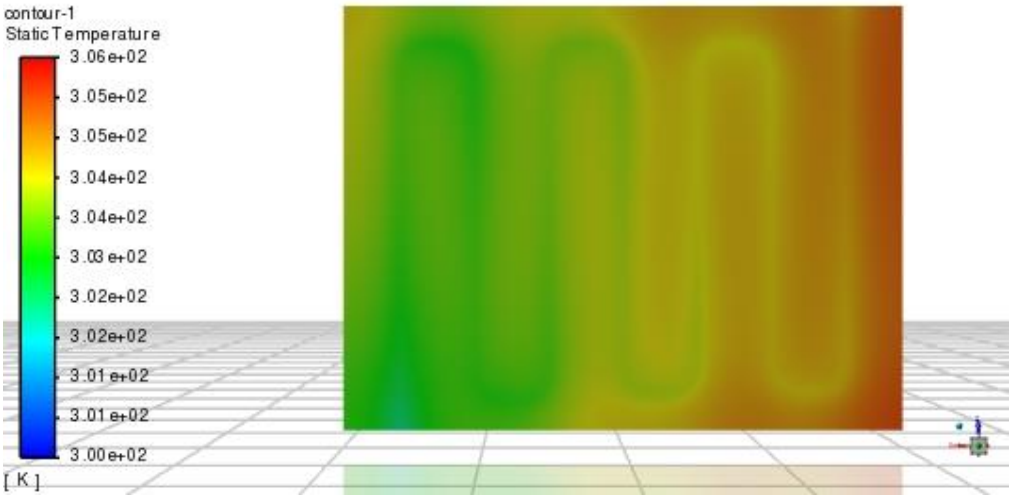

Figure 4.7: Temperature contour for 0.005 kg/sec at 600 W/m^2

Here the Figure 4.7 shows the variation of the temperature distribution at 600 W/m^2 heat flux for 0.005 kg/sec mass flow rate in the Solar PV where it can be seen that the inlet section has the lower temperature compared to the outlet section. This was because the fluid flowing through the pipe carry the heat and increases the temperature when it passes through the pipe from inlet section to outlet section.

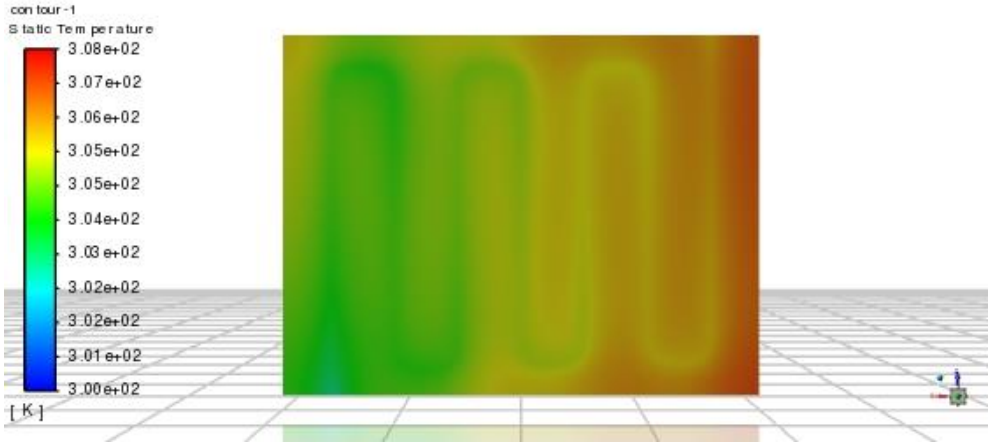

Figure 4.8: Temperature contour for 0.005 kg/sec at 800 W/m^2

Figure 4.8 shows the distribution of the temperature of Solar PV at 800 W/m^2 heat flus for 0.005 kg/sec mass flow rate. Here, it can be that the outlet section has higher temperature than the inlet section because of the flow fluid taking the heat from the panel when it flows from inlet to outlet section. The inlet section has the minimum temperature and outlet has the maximum temperature.

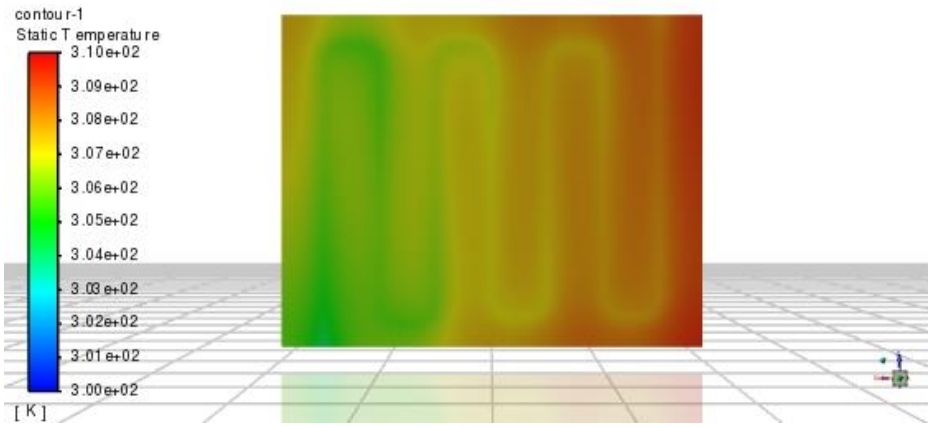

Figure 4.9: Temperature contour for 0.005 kg/sec at 1000 W/m^2

Figure 4.9 shows the temperature contour for 0.005 kg/sec mass flow rate at 1000 W/m^2 heat flux where the temperature is higher at the outlet section compared to the inlet and middle section of the solar panel. This was because of the transfer of the heat from the panel to the flowing fluid which carry the heat from the panel thus generating the thermal energy and providing the cooling effect to the panel.

On comparing the temperature contour for all the heat flux rate, similar pattern has been observed the distribution of the heat is uniform through the cell which was due to the

heat carried out by the flowing fluid thus providing the cooling effect to the cell. Because of the flowing fluid which carries the heat, the inlet section has the lower temperature compared to the outlet section as seen in the contour.

Table 4.2 shows the average cell temperature of the solar PV at different mass flow rate and heat flux rate. It also shows the electrical efficiency of the system for various flow rate at different heat flux rate.

Table 4.2: Electrical efficiency and average cell temperature at various heat flux and mass flow rate

$\dot{m}$ (kg/sec)	G=600 W/m^2		G=800 W/m^2		G=1000 W/m^2	
	T_{cell} (K)	η_{el} (%)	T_{cell} (K)	η_{el} (%)	T_{cell} (K)	η_{el} (%)
0.001	9.489	10.66%	12.652	10.02%	15.815	9.38%
0.002	6.763	11.34%	9.017	10.93%	11.271	10.52%
0.003	5.620	11.63%	7.493	11.31%	9.366	11.00%
0.004	4.958	11.79%	6.611	11.53%	8.264	11.26%
0.005	4.559	11.87%	6.078	11.64%	7.598	11.40%

The tabulated result shows that when the mass flow rate was increased then there was decrease in the cell temperature i.e., cell temperature was inversely proportional to the mass flow rate of the fluid. The electrical efficiency ranges from 9.38% to 11.87% and was maximum for 600 W/m^2 compared to the 800 and 1000 W/m^2. The electrical efficiency was found to be above one-tenth of the incident energy.

The reference efficiency, temperature coefficient of open circuit voltage was taken as 13.071% and -0.27%/K respectively at STC condition as provided by the manufacture i.e., luminous technologies Pvt. Ltd. as mentioned in the previous section.

Figure 4.10 shows the variation of the cell temperature and the electrical efficiency of the PV module with the mass flow rate.

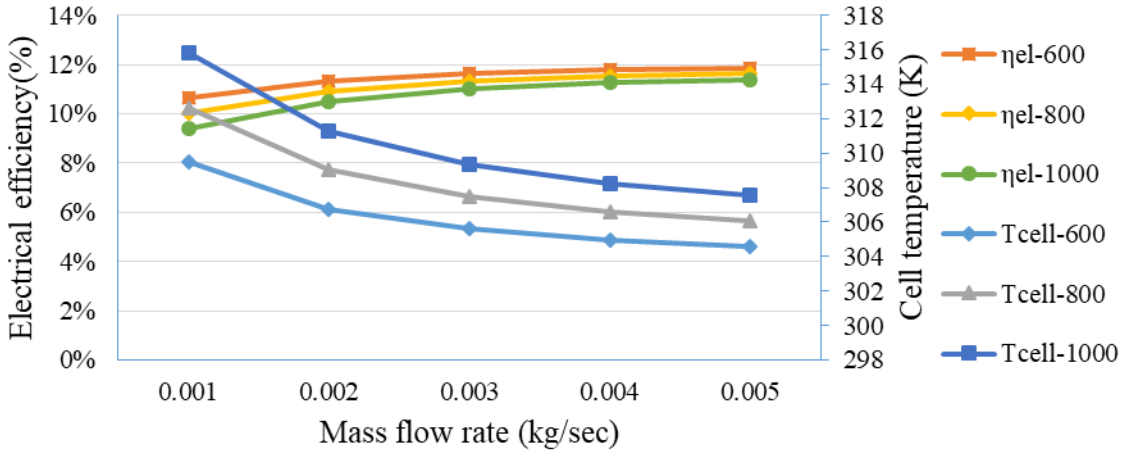

Figure 4.10: Variation of electrical efficiency and cell temperature with mass flow rate for various heat flux rate

The graphs shows that the electrical efficiency increases with increase in the mass flow rate. Similarly, the pattern of electrical efficiency is similar for all the heat flux rate where electrical efficiency was slightly higher for 600 W/m^2 heat flux compared to other followed by 800 W/m^2 and 1000 W/m^2 respectively. However, the average cell temperature was higher for higher heat flux rate i.e., higher for 1000 W/m^2 followed by 800 W/m^2 and 600 W/m^2 respectively.

The electrical efficiency obtained from CFD analysis here in this study vary from 9.38% to 11.87%. When comparing this efficiency with the result obtained by (Dupeyrat et al., 2011) and (Allan, n.d., 2015) whose value were 8.7% and 8% respectively, it was found that the electrical efficiency was nearly 26% and 32% higher respectively compared to (Dupeyrat et al., 2011) and (Allan, n.d., 2015). Similarly, when comparing with the result given by (Misha et al., 2020) and (Herrando et al., 2019), the electrical efficiency was 3% higher and 1% lower respectively.

Furthermore, comparing the result with (Dubey & Tay, 2013) shows that the electrical efficiency was only 3% higher. The variation in electrical efficiency with literature review may be due to the system design and variation in assumptions made during the CFD analysis of the system.

4.1.6 Overall efficiency

Overall efficiency was calculated by adding the thermal and electrical efficiency of the system as mentioned in the earlier section. However, some researcher considers electrical efficiency as more valuable compared to thermal energy. Therefore, they had

introduced energy saving efficiency to determine the overall performance of the system. But in this study, thermal and electrical efficiency were added to determine the overall efficiency of the system which varies from 41% to 72%. The Table 4.3 shows the comparison of the overall efficiency for different heat flux rate.

Table 4.3: Comparison of overall efficiency for various heat flux

$\dot{m}$ (kg/sec)	Overall efficiency, η_o (%)		
	G=600 W/m^2	G=800 W/m^2	G=1000 W/m^2
0.001	42.97%	42.33%	41.70%
0.002	52.87%	52.55%	52.14%
0.003	59.43%	59.13%	58.82%
0.004	64.78%	64.54%	64.29%
0.005	71.41%	70.91%	70.73%

From the Table 4.3, it was observed that the overall efficiency was higher for 600 W/m^2 which was followed by 800 W/m^2 and 1000 W/m^2 respectively. The overall efficiency at 600 W/m^2 with 0.005 kg/sec flow rate is nearly about 1 % higher than that of 1000 W/m^2 for 0.005 kg/sec flow rate. Similarly, it was almost 0.70% higher than for 800 W/m^2 heat flux with 0.005 kg/sec flow rate.

While comparing the overall efficiency obtained from the CFD analysis in this study with the literature, it was found that the results align with literature. The overall efficiency vary from 41.70% to 71.41% here in this study while the result obtained by (Dupeyrat et al., 2011) and (Allan, n.d., 2015) were 87.7% and 59% respectively which was nearly 22% lower and 17.37% higher respectively.

Further, the overall efficiency obtained here in this study when compared with the result obtained by (Herrando et al., 2019) which was in the range of 77.9 to 80.4 % was nearly 12.5% less. Likewise when comparing the result with (Yang et al., 2018) shows that the overall efficiency was almost 8.5% higher than that of (Yang et al., 2018). Moreover the result of (Misha et al., 2020) shows the overall efficiency of 71.31% which indicate that the result of this study align with (Misha et al., 2020).

However, there was certain deviation in the results with the literature which may be due to size of the system, system design and meteorological data which were different for each study. This shows that while designing the model, optimal size should be chosen to obtain the desire result.

4.2 Experimental results

Experimental setup was constructed using the polycrystalline solar panel of 20W, copper plate of thickness of 1 mm as thermal absorber, copper pipe of 10 mm OD and 9 mm ID as thermal collector and all these components were insulated and framed together. The experiment was conducted from 11:00 AM to 01:30 PM for 7 days on a sunny day. Different parameters such as inlet and outlet temperature of water, surface temperature of PV and PVT system, current and voltage of PV and PVT system and global irradiance were recorded at an interval of 30 minutes for different flow rate ranging from 60 ml/minute to 300 ml/minute i.e., (0.001 kg/sec to 0.005 kg/sec). The detail results obtained from the experiment is discussed in this section.

4.2.1 Experimental thermal efficiency

For determining the thermal efficiency, inlet and outlet temperature of working fluid i.e., water in this study was recorded using k-type thermocouple for different mass flow rate as the thermal efficiency is based on the temperature difference between inlet and outlet of the water. As there is fluctuation of the temperature of the inlet and outlet so the average temperature was taken by recording the temperature at an interval of 1 minute to minimize the error and maximize the accuracy of the measured data. The Table 4.4 shows the detail result obtained from the experiment for thermal efficiency

Table 4.4: Experimental thermal efficiency

$\dot{m}$ (kg/sec)	T_{in} (K)	T_{out} (K)	ΔT (K)	η_{th} (%)
0.001	299.143	307.643	8.500	28.522%
0.002	300.571	306.429	5.857	38.247%
0.0033	301.929	305.857	3.929	42.330%
0.004	303.786	307.286	3.500	46.524%
0.005	304.714	308.000	3.286	53.569%

From Table 4.4, it was observed that the thermal efficiency varies from 28.522% to 53.569%. There was an increase of 34% of thermal efficiency when the mass flow changes from 0.001 kg/sec to 0.002 kg/sec which was maximum increase in the thermal efficiency. Moreover, it was observed that overall thermal efficiency increased by almost 87% when flow rate increased from 0.001 kg/sec to 0.005 kg/sec. Further, the temperature difference decreases from 8.5K to 3.286K.

Figure 4.11 shows how the thermal efficiency and temperature difference vary with various mass flow rate recorded during the experiment.

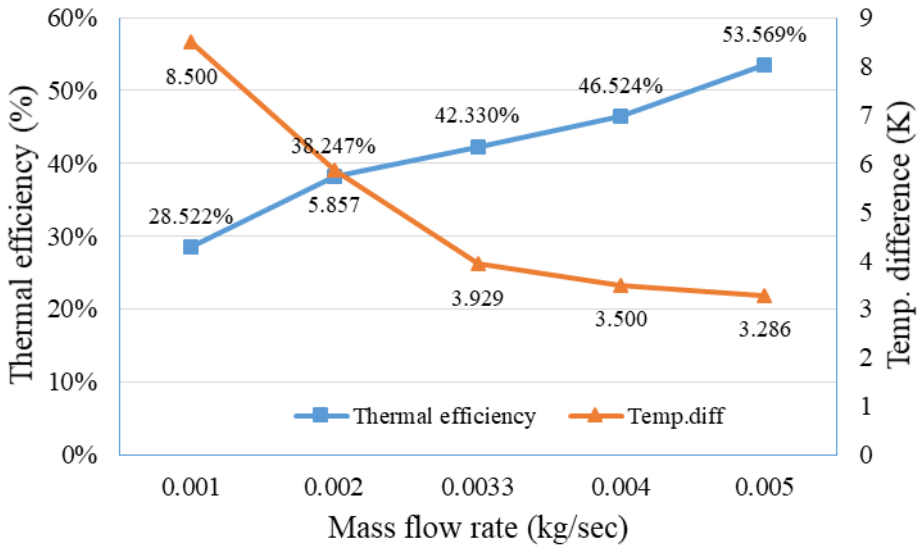

Figure 4.11: Relation of temperature difference and thermal efficiency with mass flow rate –experimental data

From Figure 4.11, it was noted that, as the mass flow rate increases the thermal efficiency is increasing. Similarly, it was also found that the temperature difference was decreasing with increased mass flow rate. With the decrease of 5.214K there was nearly 87% increases in the thermal efficiency with increase in the mass flow rate.

When comparing this result with (Yang et al., 2018), it was found that the thermal efficiency obtained from the experiment was nearly 9% lower while it was 30% higher when compared with the result obtained from (Dubey & Tay, 2013).

Similarly, when compared with (Herrando et al., 2019), the thermal efficiency was nearly 24% lower. Overall, the thermal efficiency obtained from the experiment align with the result obtained by the previous researcher. The variation when comparing with the literature was because of the materials used for the experiment, the assumptions made during each study and the meterlgological data as the study was conducted in various parts of the world.

4.2.2 Experimental electrical efficiency

Electrical efficiency of both the system i.e., PV and PVT were determined by measuring the current and voltage of each system using the multimeter. During the experiment current and voltage are continuously measured through the multimeter and average value were taken for each mass flow rate at the interval of 1 minute.

Figure 4.12 shows the comparison of electrical power for PV system and PVT system calculated from experiment.

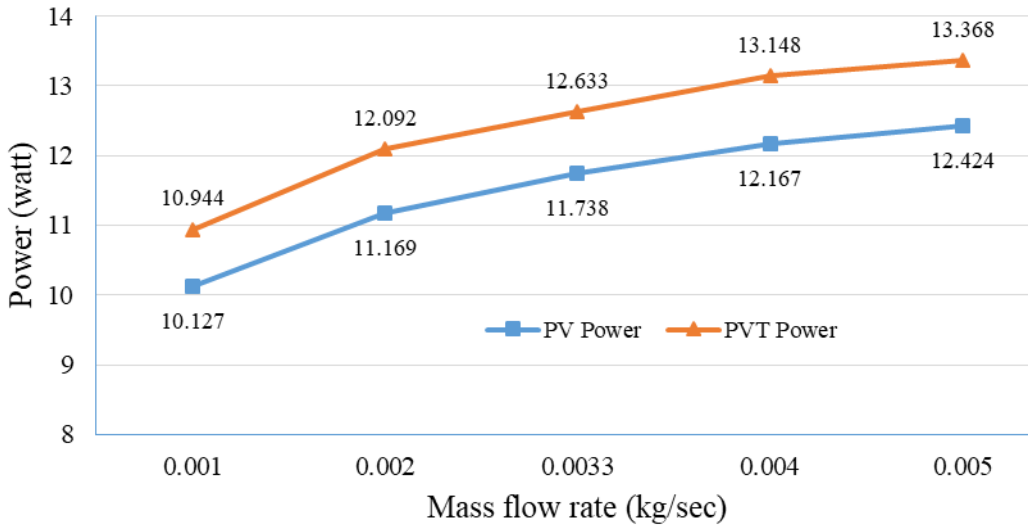

Figure 4.12: Comparison of electrical power for PV and PVT system

From Figure 4.12, it was clear that the power was higher for PVT system compared to the PV system. The power varies from 10.127 watt to 12.424 watt for PVT system while it varies from 10.944 watt to 13.368 watt for PVT system. The deviation varies from 7% to 8% and this variation was because of the heat carried out by the flowing fluid in the PVT system which cools the cell temperature of the PVT system compared to the PV system thus increasing the current and voltage of the system. This also indicate that when the cell temperature decreases then the power increases. Further, it can be seen that the power increases with increase in the flow rate and both follow the similar trend.

Table 4.5: Comparison of electrical efficiency for PVT and PV system

ṁ (kg/sec)	Electrical efficiency (ηele %)	
	PVT	PV
0.001	8.781%	8.127%
0.002	9.440%	8.722%
0.0033	9.865%	9.170%
0.004	10.453%	9.673%
0.005	10.430 %	9.697%

From the above table, it was seen that the electrical efficiency varies from 8.781% to 10.453% for PVT system while it ranges from 8.127% to 9.697% for PV system. It was also analyzed that the electrical efficiency for PVT system was higher compared to PV system. This is due to the heat dissipation of the PVT system which is carried by the

flowing fluid in the collector which provides the cooling effect to the PVT system. However, in both cases the electrical efficiency is increasing with the increases mass flow rate. The deviation of the electrical efficiency between PVT and PV system varies from 7.58% to 8.23% which indicates that the PVT system help to increase the electrical power compared to the PV system alone by providing the cooling effect to the system.

Figure 4.13 shows the effect of mass-flow rate in electrical efficiency and temperature difference for experimental data.

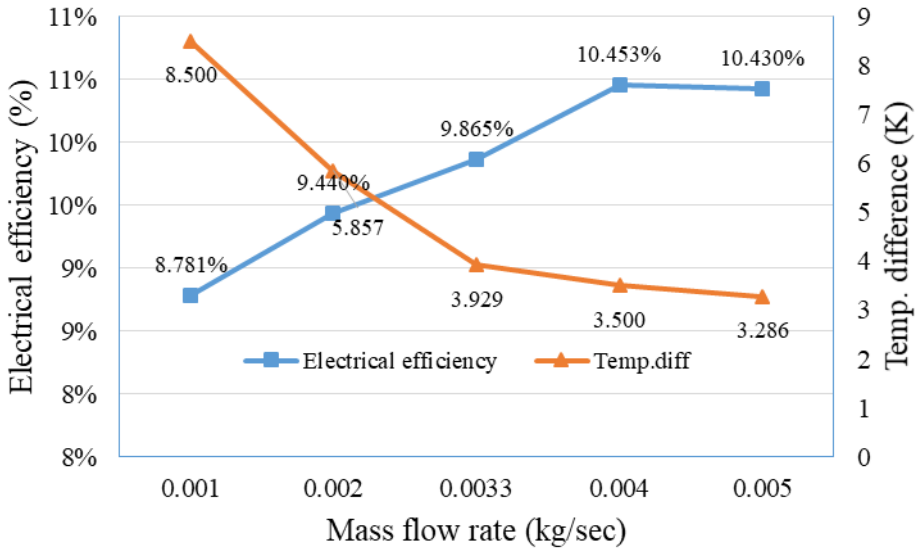

Figure 4.13: Relation of temperature difference and electrical efficiency with various mass flow rate-experimental data

From Figure 4.13, it was analyzed that the electrical efficiency rises with rise in flow rate while the difference in temperature between inlet and outlet fall with rise in flow rate. This trend was similar to that of the thermal efficiency and temperature difference with the mass flow rate. There was an overall rise of 19% in electrical efficiency when the mass flow rate increases from 0.001 kg/sec to 0.005 kg/sec with a decrease of 5.214K.

Figure 4.14 shows the electrical efficiency for PVT system and PV alone system calculated during experiment.

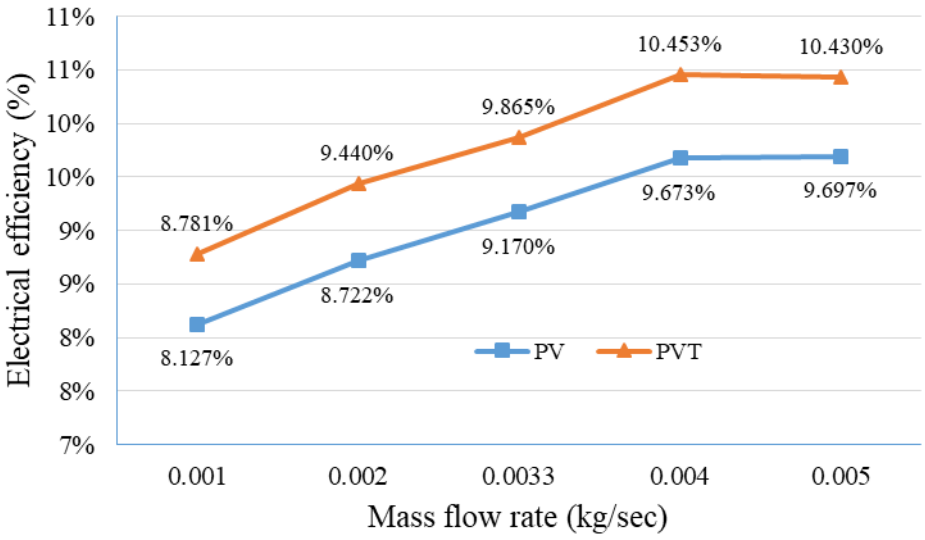

Figure 4.14: Comparison of electrical efficiency for PVT and PV system

From Figure 4.14, it was observed that the trend of the electrical efficiency was similar in both cases i.e., for PVT and PV. There was variation in the efficiency which was due to the transfer of heat from the cell to the flowing fluid thus cooling the panel in case of PVT system compared to the PV system.

Figure 4.15 shows the effect of flow rate on the average cell temperature of the PV system and PVT system measured during seven days experiment.

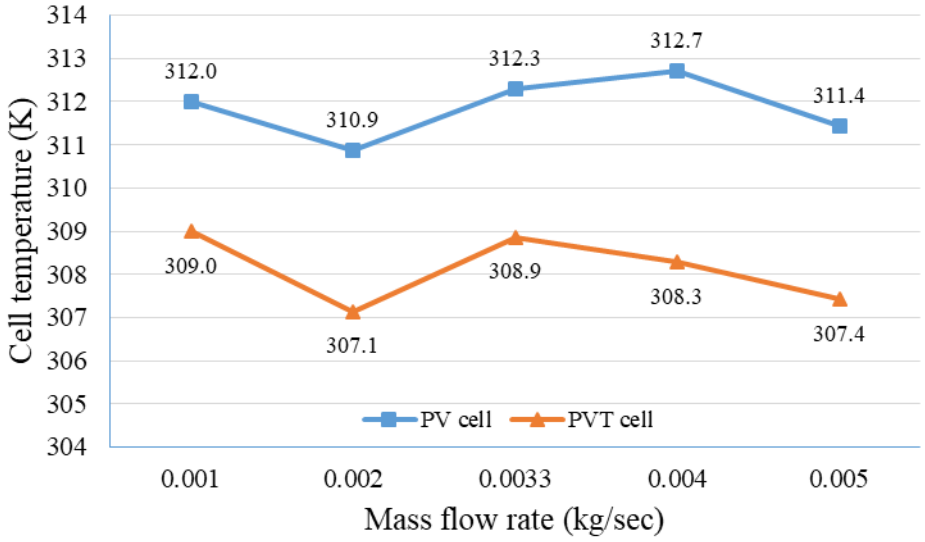

Figure 4.15: Variation of cell temperature for PV and PVT system

From Figure 4.15, it was noted that the cell temperature for PV system was higher than that of the PVT system. It was also analyzed that for PVT system the cell temperature decreases when the flow rate increase from 0.001 kg/sec to 0.002 kg/sec and then increases upto 0.003 kg/sec. Afterward the cell temperature decreases with the flow rate. However, the trend was slightly different in case of PV system where it can be seen that the cell temperature first decreases and then increases upto 0.004 kg/sec flow rate and then again decreases afterward. It was also analyzed that the deviation of the cell temperature between PV and PVT system varies from 0.9% to 1.4% which indicates that the flowing fluid gets heated thus decreasing the cell temperature of the PVT system compared to the PV system.

The variation in the trend of the cell temperature between the PV and PVT system may be due to the higher value of solar intensity with respect to time, as the solar intensity change with respect to time. This shows that the PVT system generate the thermal energy and provide the cooling effect to the system thus improving the electrical performance of the system.

While comparing the electrical efficiency with (Misha et al., 2020) result, it was analyzed that the electrical efficiency obtained here in this study was nearly 12% lower. Similarly the electrical efficiency obtained in this study was 10% lower compared to the result obtained by (Dubey & Tay, 2013). When compared with (Herrando et al., 2019), it was almost 14.8% lower which indicates that the electrical efficiency determined here in this study align with the electrical efficiency determined by the previous researcher. The variation in the result may be due to the material properties used, climatic condition at which the experiment was conducted and the type of solar PV used for preparing the PVT system.

4.2.3 Experimental overall efficiency

Figure 4.16 shows the variation of experimental overall efficiency. Here the overall efficiency was obtained by adding thermal efficiency with electrical efficiency.

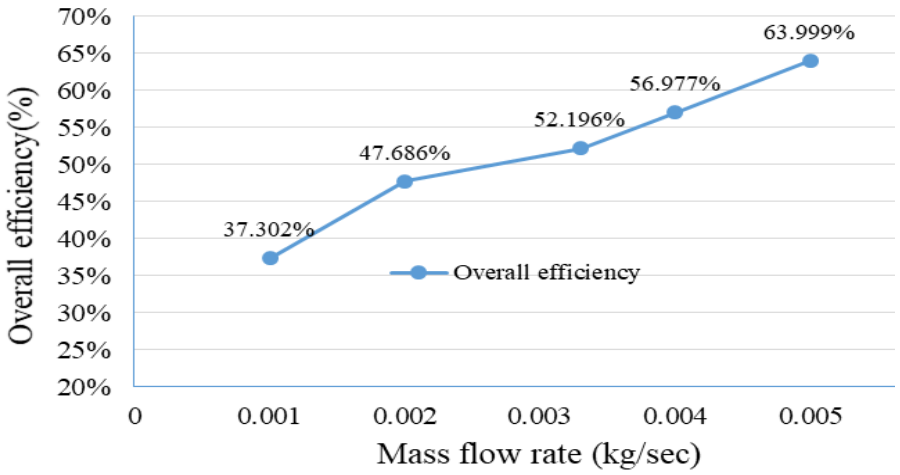

Figure 4.16: Variation of overall efficiency for experiment

From Figure 4.16, it was analyzed that the overall efficiency rises with rise in flow rate. Overall efficiency ranges from 37.302% to 63.999% showing rising trend with flow rate. It was found that the overall efficiency increases by nearly 28% when the flow rate increased from 0.001 kg/sec to 0.002 kg/sec. The overall increment of the overall efficiency is nearly 1.71 times when the mass flow rate increased from 0.001 kg/sec to 0.005 kg/sec.

To validate the result obtained in this study, the result obtained was compared with several literature. When compared the result with (Yang et al., 2018), it shows the variation of 2% i.e., the overall efficiency obtained in this study was lower by 2%. Similarly, when compared with (Misha et al., 2020), again the overall efficiency was lower by 11%. However, when compared with (Dubey & Tay, 2013), the overall efficiency obtained here in this study was higher by 20%. This variation in overall efficiency when compared with various literature was because of the climatic conditions where the experiment was conducted, material used for experimental setup and the type of solar PV used for preparing the PVT system.

4.3 Comparison of CFD and experimental results

Here in this section, the results obtained from the simulation and experiment were compared. During the comparison, the results of simulation for 800 W/m^2 was taken because while conducting the experiment the global irradiance varying in the range of 760-860 W/m^2. For comparison different parameters such as thermal efficiency, electrical efficiency and overall efficiency, temperature difference between inlet and outlet, electrical power was compared.

a. Comparison of thermal efficiency

Figure 4.17 shows the variation of the thermal efficiency obtained from simulation and experiment.

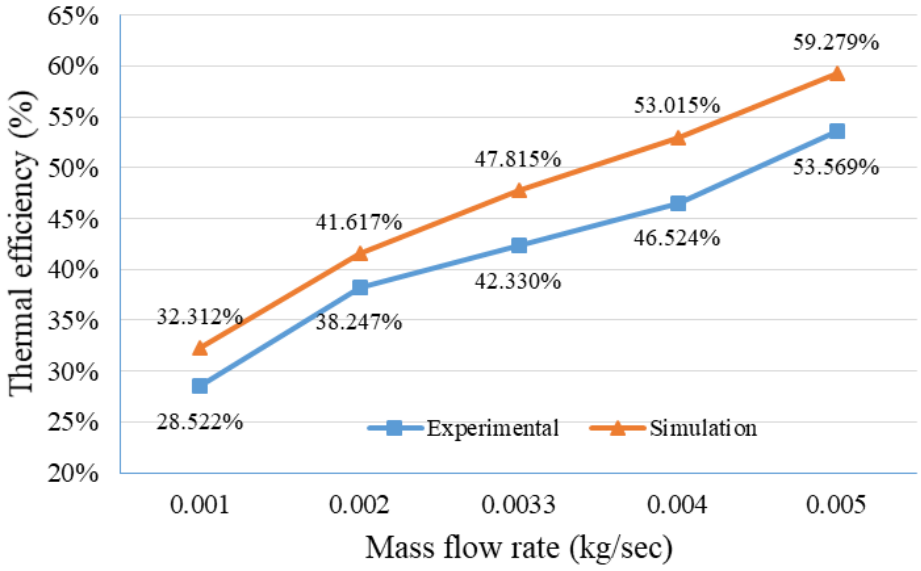

Figure 4.17: Comparison of thermal efficiency –experimental and simulation

From Figure 4.17, it was observed that the both approach has similar trend of thermal efficiency i.e., in both cases thermal efficiency was increasing with increase in the flow rate. From the simulation it was found that the thermal efficiency varies from 32.212% to 59.279% while it ranges from 28.522% to 53.569% for experiment.

When analyzing the result from simulation and experiment, it was observed that the deviation was in between 8% to 14% with maximum deviation at 0.004 kg/sec mass flow rate. This deviation may be due to varying meteorological data, geographical conditions, variation in assumption made for CFD, losses to surroundings and instrument inaccuracy. It was also observed that when the mass flow rate increases from 0.001 kg/sec to 0.002 kg/sec then the increase in thermal efficiency was maximum in both cases compared to other flow rate.

b. Comparison of temperature difference

Figure 4.18, shows the result for temperature difference between the inlet and outlet of the flowing fluid obtained from simulation and experiment. During the experiment, average temperature was taken as the temperature vary with the time. Therefore, the

temperature was noted for 1 minute and then average value was taken for the calculation in both inlet and outlet for the experiment data.

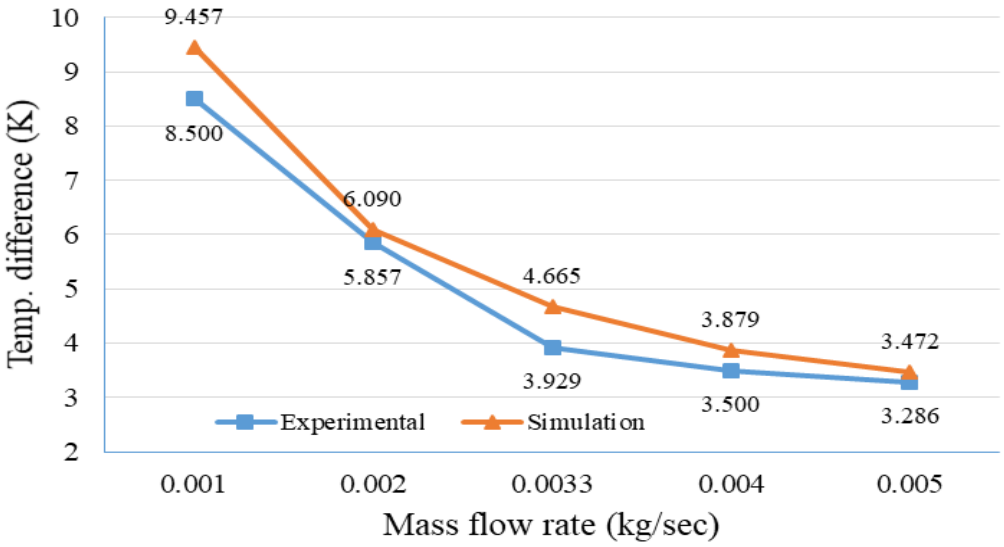

Figure 4.18: Comparison of temperature difference-experimental and simulation

From Figure 4.18, it was found that the temperature difference for simulation data was more compared to the experimental result. This was because during the simulation, the inlet temperature and heat flux was kept constant for certain flow rate but during the experiment the solar irradiance vary with the time and the inlet temperature and outlet temperature of water also vary with the time.

The results show that the difference in outlet water temperature decreases with increases mass flow rate. It can be seen that at low speeds the outlet temperature difference was higher. This is because, at low speeds, the rate of heat removal from the tube is much higher than the rates of heat obtained from the PV module.

Furthermore, at higher flow rate the volume of water gets contact to the tube wall for very less time to accumulate thermal energy, thus reducing the water outlet temperature. Almost 19% deviation was observed for 0.003 kg/sec flow rate while minimum deviation was nearly 4% for 0.002 kg/sec. However, it was also analyzed that the temperature difference between the inlet and outlet decreases with increase in the flow rate and has similar trend in both cases.

c. Comparison of electrical efficiency

Figure 4.19 shows the comparison of electrical efficiency between the simulation and experiment.

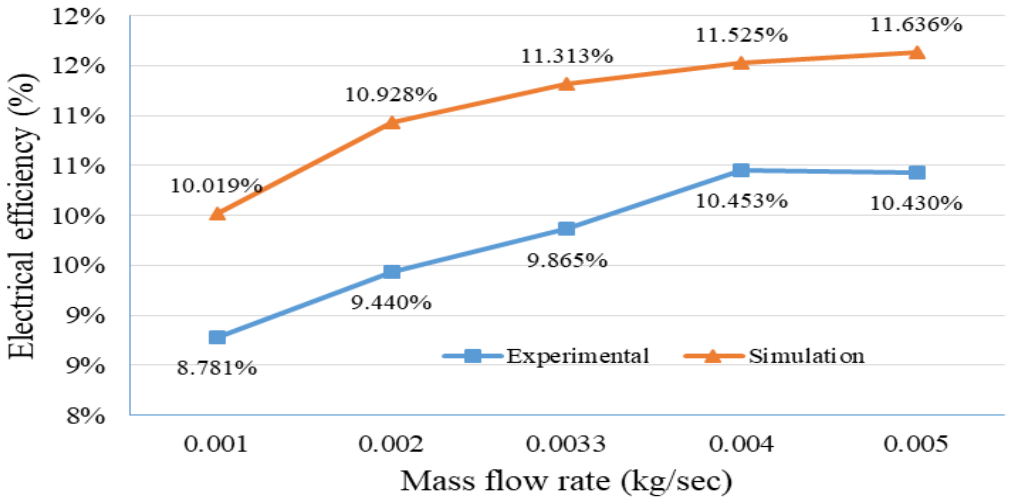

Figure 4.19: Comparison of electrical efficiency-experimental and simulation

From Figure 4.19, it was seen that the simulation has higher electrical efficiency in comparison to experimental results. The simulation result shows that the electrical efficiency varies from 10.019% to 11.636% whereas the experimental efficiency varies from 8.781% to 10.430%. It was also observed that the efficiency was increasing with increase in flow rate. Nearly difference of 1.6% of electrical efficiency was observed in both simulation and experimental with expense of 5.214K decrease in temperature for experiment and 5.985K for simulation respectively.

However, there was deviation in the electrical efficiency between simulation and experimental. The deviation varies from 10% to 16% which was observed due to varying meteorological data, geographical conditions such as varying global irradiance with respect to time, variation in assumptions made for CFD and losses to surroundings. Moreover, both simulation and experimental results shows the similar trend and has similar pattern of electrical efficiency with respect to mass flow rate.

d. Comparison of overall efficiency

Figure 4.20 shows the comparison of overall efficiency for CFD and experimental result.

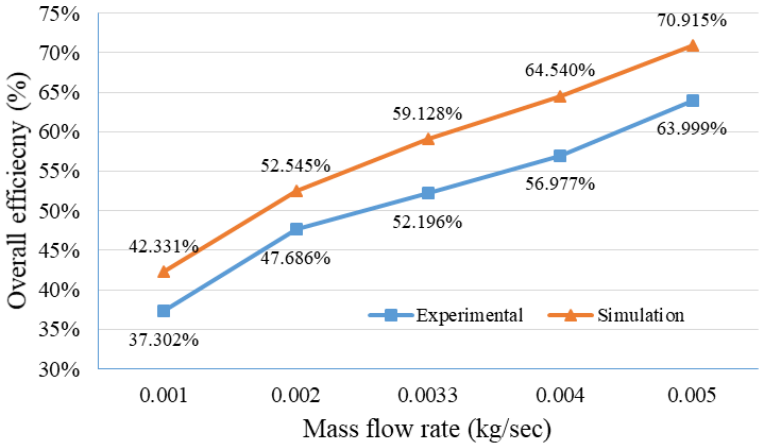

Figure 4.20: Comparison of overall efficiency –experimental and simulation

From Figure 4.20, it was analyzed that the simulation result has higher overall efficiency compared to the experimental result. The graph shows that the overall efficiency varies from 42.331% to 70.915% during CFD analysis while it ranges from 37.302% to 63.999% during experimental analysis. The maximum and minimum deviation were found to be 13.643% and 10.242% respectively. The reason behind the deviation may be due to varying meteorological data, geographical conditions such as varying global irradiance with respect to time, variation in assumptions made for CFD and losses to surroundings. Moreover, both simulation and experimental results shows the similar trend and has similar pattern of overall efficiency with respect to mass flow rate.

e. Comparison of cell temperature

Figure 4.21 shows the comparison of experimental and simulation cell temperature.

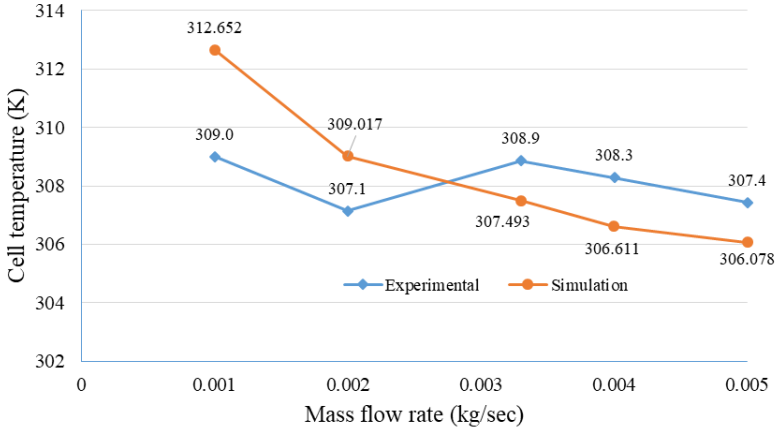

Figure 4.21: Comparison of cell temperature –experimental and simulation

From Figure 4.21, it was analyzed that the cell temperature for simulation decreases with increase in flow rate but in case of experiment, the cell temperature first decreases and increases and then again decreases with increase in flow rate. This unusual behavior in the cell temperature in experiment was due to change in the value of global irradiance, meteorological data and variation in assumption made for the CFD. As the cell temperature is directly affected by the amount of irradiance fall on the face of the solar PV and during the experiment the intensity of the solar irradiance vary with respect to time.

However, in case of simulation the value of solar intensity was kept constant to 800W/m^2 with inlet temperature at 300K. This is why there was unusual behavior in the cell temperature in experiment and decreasing trend in simulation. For simulation the value decreases from 312.652K to 306.078K while it varies from 309.0K to 307.4K in case of experiment as seen in the figure above.

f. Comparison of thermal efficiency with respect to heat loss parameter

Figure 4.22 shows the comparison of thermal efficiency with respect to heat loss parameter.

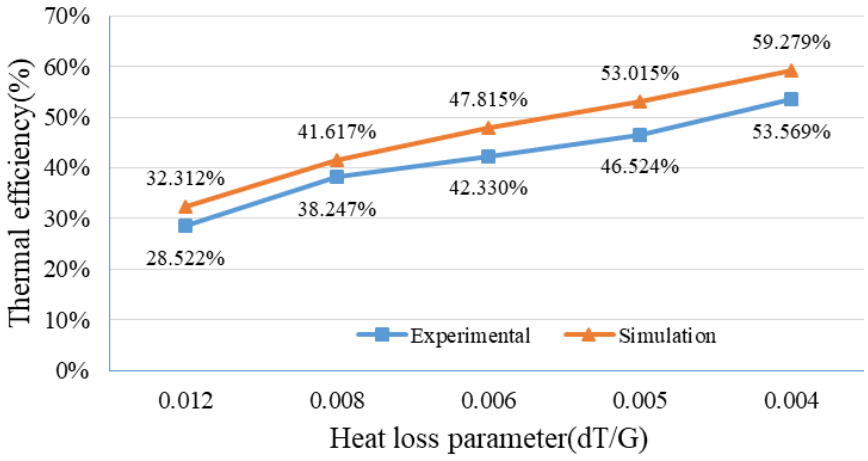

Figure 4.22: Comparison of variation of thermal efficiency with heat loss parameter-experimental and simulation

From Figure 4.22, it was observed that the thermal efficiency increases with decreases in the heat loss parameter. However, there was deviation between the simulation and experimental result which may be due to varying meteorological data, geographical conditions such as varying global irradiance with respect to time, variation in assumptions made for CFD and losses to surroundings. Moreover, both simulation and

experimental results shows the similar trend and has similar pattern of electrical efficiency with respect to heat loss parameter.

g. Comparison of electrical efficiency with respect to heat loss parameter

Figure 4.23 shows the comparison of electrical efficiency for PVT, PV and simulation with respect to heat loss parameter.

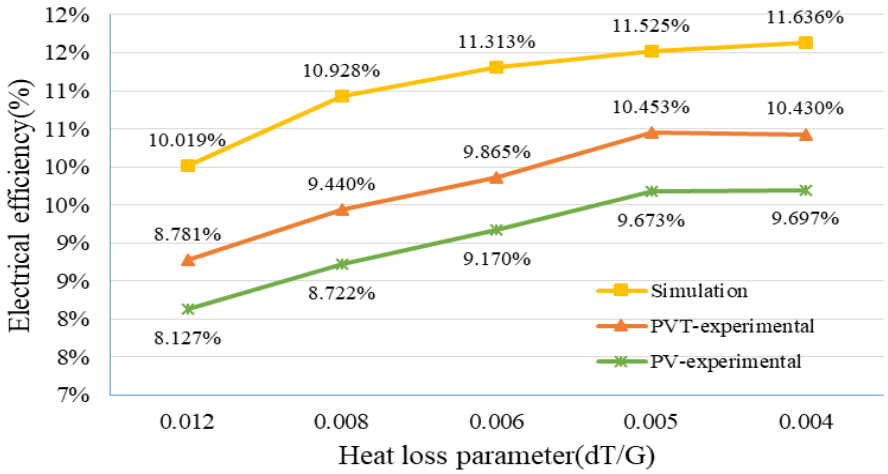

Figure 4.23: Comparison of variation of electrical efficiency with heat loss parameter-experimental and simulation

From Figure 4.23, it was clearly seen that the electrical efficiency was lower for PV system compared to the PVT system and simulation. The electrical efficiency increases with decreases in the heat loss parameter. There was no so much deviation in electrical efficiency between PV and PVT system when compared to the simulation analysis. The deviation between the electrical efficiency was because of the varying global irradiance during the experiment which causes to vary the voltage and current.

Similarly, the flowing fluid took away the heat from the panel which provides the cooling effect to the system thus decreasing the temperature of the cell and increasing the electrical efficiency. However, for the deviation between simulation and experimental result it may be due to varying meteorological data, geographical conditions such as varying global irradiance with respect to time, variation in assumptions made for CFD and losses to surroundings. Moreover, both simulation and experimental results shows the similar trend and has similar pattern of electrical efficiency with respect to heat loss parameter.

CHAPTER FIVE: CONCLUSIONS AND RECOMMENDATIONS

5.1 Conclusions

Following conclusions has been drawn from the study;

- Outlet temperature of water and cell temperature decreases with increase in the mass flow rate and heat flux and was maximum at 0.001 kg/sec mass flow rate at 1000 W/m^2
- The average highest value of cell temperature of PVT system and PV system were 309.0K and 312.7K at mass flow rate of 0.001 and 0.004 kg/sec respectively
- The CFD analysis revealed that the system's thermal efficiency ranged from 32.312% to 59.279%, while on the experimental side, its value ranges from 28.522% to 53.569% with maximum deviation of 14% at 0.004 kg/sec mass flow rate
- The CFD analysis revealed that the system's electrical efficiency ranged from 10.019% to 11.636%, while on the experimental side it ranges from 8.781% to 10.453% with maximum deviation of 16% at 0.002 kg/sec mass flow rate
- The CFD analysis indicated that the overall efficiency ranged from 42.331% to 70.915%, while experimental analysis showed a range of 37.302% to 63.999% with maximum deviation of nearly 14% at 0.001 kg/sec mass flow rate
- Cooling effect was observed which help to increase the electrical efficiency of the system because of the heat carried out by the flowing fluid

5.2 Recommendations

Following recommendation can be provided;

- An examination can be carried out to assess the impact of an extremely high flow rate in order to determine the mass flow rate that maximizes energy transfer. For this study, the flow rate has been limited to 0.005 kg/sec
- Experiment can be carried out by varying the geographical location to understand the variation of performance of the system
- Further study can be carried out by varying the diameter of the thermal collector to find the optimal size of the collector which help to improve the system's performance

- The effect of incorporating various storage systems for electrical energy (such as batteries) and thermal energy (like a water tank with a heat exchanger) can be investigated to understand the fluctuations in efficiency. This analysis could be performed based on factors like building integration and concentrated solar power, potentially resulting in improved efficiency and adaptability of solar energy systems.

REFERENCE

Abdul-Ganiyu, S., Quansah, D. A., Ramde, E. W., Seidu, R., & Adaramola, M. S. (2021). Techno-economic analysis of solar photovoltaic (PV) and solar photovoltaic thermal (PVT) systems using exergy analysis. *Sustainable Energy Technologies and Assessments*, *47*, 101520. https://doi.org/10.1016/j.seta.2021.101520

Allan, J. (n.d.). *The Development and Characterisation of Enhanced Hybrid Solar Photovoltaic Thermal Systems*.

Arslan, E., Aktaş, M., & Can, Ö. F. (2020). Experimental and numerical investigation of a novel photovoltaic thermal (PV/T) collector with the energy and exergy analysis. *Journal of Cleaner Production*, *276*, 123255. https://doi.org/10.1016/j.jclepro.2020.123255

Assoa, Y. B., Menezo, C., Fraisse, G., Yezou, R., & Brau, J. (2007). Study of a new concept of photovoltaic–thermal hybrid collector. *Solar Energy*, *81*(9), 1132–1143. https://doi.org/10.1016/j.solener.2007.04.001

Chow, T. T. (2003). Performance analysis of photovoltaic-thermal collector by explicit dynamic model. *Solar Energy*, *75*(2), 143–152. https://doi.org/10.1016/j.solener.2003.07.001

Dubey, S., Sarvaiya, J. N., & Seshadri, B. (2013). Temperature Dependent Photovoltaic (PV) Efficiency and Its Effect on PV Production in the World – A Review. *Energy Procedia*, *33*, 311–321. https://doi.org/10.1016/j.egypro.2013.05.072

Dubey, S., & Tay, A. A. O. (2013). Testing of two different types of photovoltaic–thermal (PVT) modules with heat flow pattern under tropical climatic conditions. *Energy for Sustainable Development*, *17*(1), 1–12. https://doi.org/10.1016/j.esd.2012.09.001

Duffie, J. A., & Beckman, W. A. (2013). *Solar engineering of thermal processes*. John Wiley & Sons.

Dupeyrat, P., Ménézo, C., Rommel, M., & Henning, H.-M. (2011). Efficient single glazed flat plate photovoltaic–thermal hybrid collector for domestic hot water system. *Solar Energy*, *85*(7), 1457–1468. https://doi.org/10.1016/j.solener.2011.04.002

Herrando, M., Ramos, A., Zabalza, I., & Markides, C. N. (2019). A comprehensive assessment of alternative absorber-exchanger designs for hybrid PVT-water collectors. *Applied Energy*, *235*, 1583–1602. https://doi.org/10.1016/j.apenergy.2018.11.024

Huang, B. J. (1993). Performance rating method of thermosyphon solar water heaters. *Solar Energy*, *50*(5), 435–440. https://doi.org/10.1016/0038-092X(93)90065-V

Huang, B. J., Lin, T. H., Hung, W. C., & Sun, F. S. (2001). Performance evaluation of solar photovoltaic/thermal systems. *Solar Energy*, *70*(5), 443–448. https://doi.org/10.1016/S0038-092X(00)00153-5

Ibrahim, A., Jin, G. L., Daghigh, R., Salleh, M. H. M., Othman, M. Y., Ruslan, M. H., Mat, S., & Sopian, K. (2009). Hybrid Photovoltaic Thermal (PV/T) Air and Water Based Solar Collectors Suitable for Building Integrated Applications.

American Journal of Environmental Sciences, *5*(5), 618–624. https://doi.org/10.3844/ajessp.2009.618.624

Islam, M. M., Pandey, A. K., Hasanuzzaman, M., & Rahim, N. A. (2016). Recent progresses and achievements in photovoltaic-phase change material technology: A review with special treatment on photovoltaic thermal-phase change material systems. *Energy Conversion and Management*, *126*, 177–204. https://doi.org/10.1016/j.enconman.2016.07.075

Jaeger, J. (2021). *Explaining the Exponential Growth of Renewable Energy*. https://www.wri.org/insights/growth-renewable-energy-sector-explained

Jordan, D. C., & Kurtz, S. R. (2013). Photovoltaic Degradation Rates-an Analytical Review: Photovoltaic degradation rates. *Progress in Photovoltaics: Research and Applications*, *21*(1), 12–29. https://doi.org/10.1002/pip.1182

Kalogirou, S. A. (2001). Use of TRNSYS for modelling and simulation of a hybrid pv–thermal solar system for Cyprus. *Renewable Energy*, *23*(2), 247–260. https://doi.org/10.1016/S0960-1481(00)00176-2

Kalogirou, S. A., & Tripanagnostopoulos, Y. (2006a). Hybrid PV/T solar systems for domestic hot water and electricity production. *Energy Conversion and Management*, *47*(18–19), 3368–3382. https://doi.org/10.1016/j.enconman.2006.01.012

Kalogirou, S. A., & Tripanagnostopoulos, Y. (2006b). Hybrid PV/T solar systems for domestic hot water and electricity production. *Energy Conversion and*

Management, *47*(18–19), 3368–3382. https://doi.org/10.1016/j.enconman.2006.01.012

Karunasena, U., Karunarathna, M. A. P., Kumara, D., Manthilake, M., & Punchihewa, H. K. G. (2020). Efficiency Improvement of Solar Photovoltaic Thermal Systems by Experimental and Numerical Analysis. *2020 Moratuwa Engineering Research Conference (MERCon)*, 488–493.

Kern, J., & Russell, M. C. (1978). *Combined photovoltaic and thermal hybrid collector systems* (COO-4577-3; CONF-780619-24). Massachusetts Inst. of Tech., Lexington (USA). Lincoln Lab. https://www.osti.gov/biblio/6352146

Khelifa, A., Touafek, K., Ben Moussa, H., & Tabet, I. (2016). Modeling and detailed study of hybrid photovoltaic thermal (PV/T) solar collector. *Solar Energy*, *135*, 169–176. https://doi.org/10.1016/j.solener.2016.05.048

Lewis, N. S., & Nocera, D. G. (2006). Powering the planet: Chemical challenges in solar energy utilization. *Proceedings of the National Academy of Sciences*, *103*(43), 15729–15735. https://doi.org/10.1073/pnas.0603395103

Matuska, T. (2012). Simulation Study of Building Integrated Solar Liquid PV-T Collectors. *International Journal of Photoenergy*, *2012*, 1–8. https://doi.org/10.1155/2012/686393

Misha, S., Abdullah, A. L., Tamaldin, N., Rosli, M. A. M., & Sachit, F. A. (2020). Simulation CFD and experimental investigation of PVT water system under natural Malaysian weather conditions. *Energy Reports*, *6*, 28–44. https://doi.org/10.1016/j.egyr.2019.11.162

Nepal Energy Sector Synopsis Report—2022. (2022).

Poudyal, K., Bhattarai, B., Sapkota, B., & Kjeldstad, B. (2012). Solar Radiation Potential at Four Sites of Nepal. *Journal of the Institute of Engineering*, *8*. https://doi.org/10.3126/jie.v8i3.5944

Renewable Power Generation Costs in 2021. (2022, July 13). https://www.irena.org/publications/2022/Jul/Renewable-Power-Generation-Costs-in-2021

Schön, G. (2017). *NUMERICAL MODELLING OF A NOVEL PVT COLLECTOR AT CELL RESOLUTION*. http://urn.kb.se/resolve?urn=urn:nbn:se:kth:diva-212731

Tiwari, G. N., Tiwari, A., & Shyam. (2016). Solar Cell Materials, Photovoltaic Modules and Arrays. In G. N. Tiwari, A. Tiwari, & Shyam (Eds.), *Handbook of Solar Energy: Theory, Analysis and Applications* (pp. 123–170). Springer. https://doi.org/10.1007/978-981-10-0807-8_4

Tyagi, J. (2021). Advances in Alternative Sources of Energy. In *Energy* (pp. 18–54). John Wiley & Sons, Ltd. https://doi.org/10.1002/9781119741503.ch2

Wolf, M. (1976). Performance analyses of combined heating and photovoltaic power systems for residences. *Energy Conversion*, *16*(1–2), 79–90. https://doi.org/10.1016/0013-7480(76)90018-8

Xie, W. T., Dai, Y. J., & Wang, R. Z. (2013). Thermal performance analysis of a line-focus Fresnel lens solar collector using different cavity receivers. *Solar Energy*, *91*, 242–255. https://doi.org/10.1016/j.solener.2013.01.029

Yang, X., Sun, L., Yuan, Y., Zhao, X., & Cao, X. (2018). Experimental investigation on performance comparison of PV/T-PCM system and PV/T system. *Renewable Energy*, *119*, 152–159. https://doi.org/10.1016/j.renene.2017.11.094

Zondag, H. A., de Vries, D. W., van Helden, W. G. J., van Zolingen, R. J. C., & van Steenhoven, A. A. (2003). The yield of different combined PV-thermal collector designs. *Solar Energy*, *74*(3), 253–269. https://doi.org/10.1016/S0038-092X(03)00121-X

ANNEX

Table: Thermal efficiency at 600 W/m^2 for various mass flow rate

ṁ (kg/sec)	Tout (K)	ΔT (K)	Qu (Watt)	ηth (%)
0.001	307.092	7.09197	29.658	32.308%
0.002	304.558	4.55775	38.121	41.526%
0.003	303.498	3.49763	43.881	47.801%
0.004	302.908	2.90836	48.651	52.997%
0.005	302.614	2.61414	54.661	59.544%

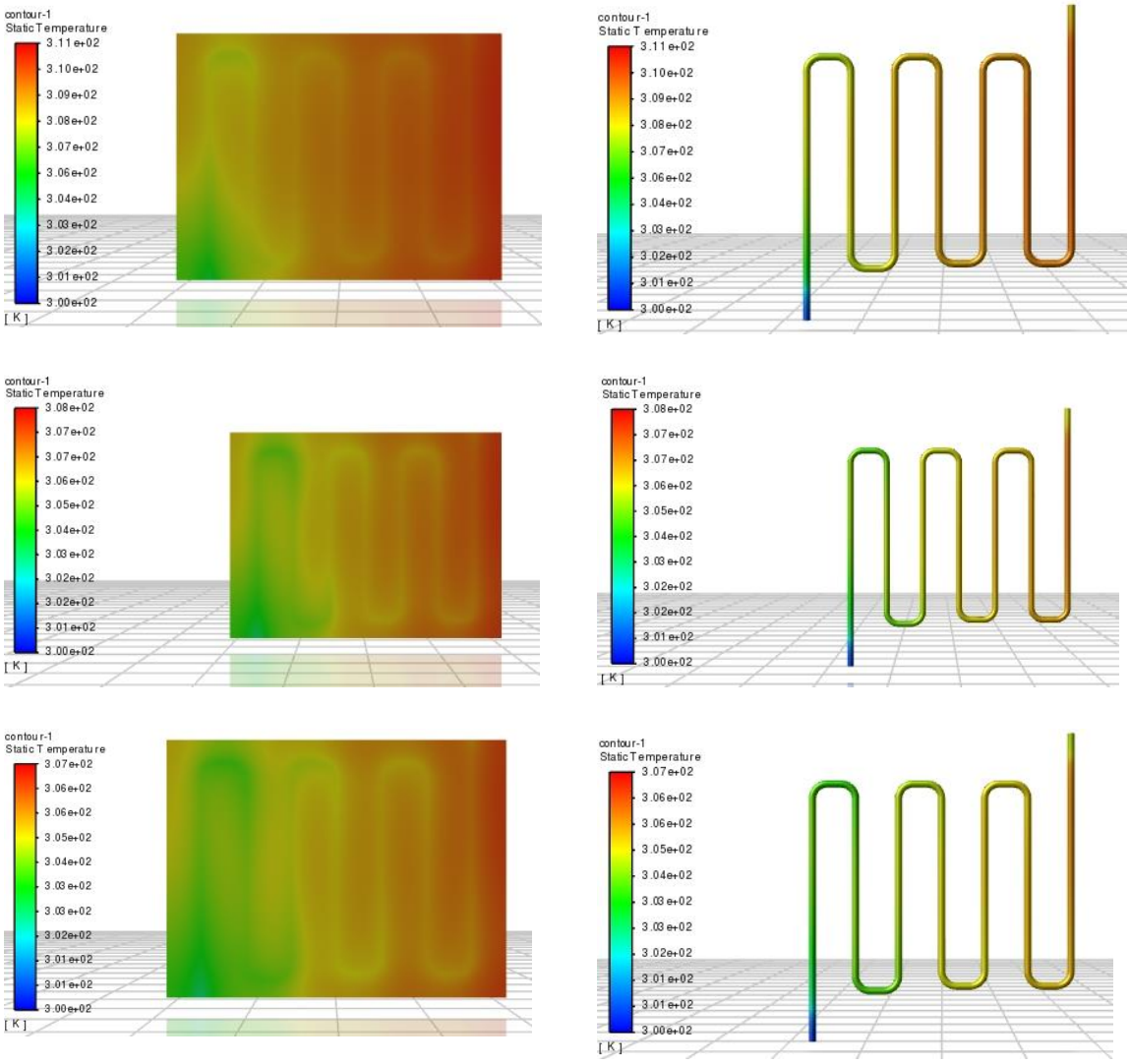

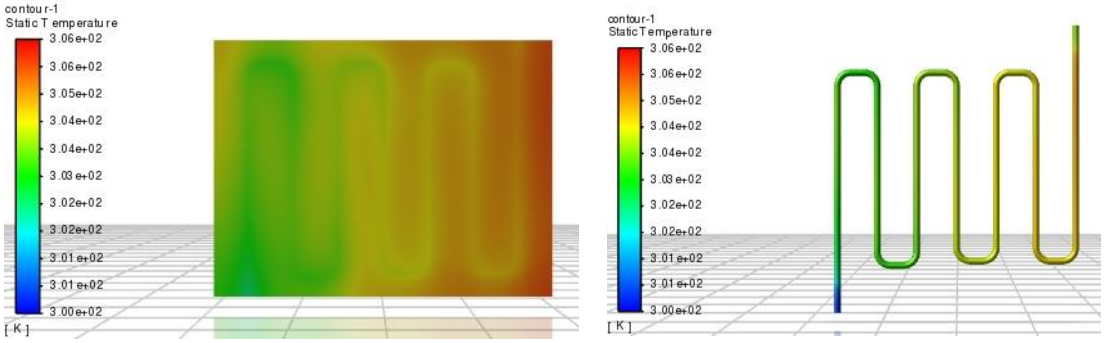

Temperature contour of PV panel and pipes for 0.001 to 0.004 kg/sec at 600 W/m^2 in sequential order

Table: Thermal efficiency at 800 W/m^2 for various mass flow rate

ṁ (kg/sec)	T_{out} (K)	ΔT (K)	Qu (Watt)	η_{th} (%)
0.001	309.457	9.457	39.550	32.312%
0.002	306.090	6.090	50.940	41.617%
0.003	304.665	4.665	58.525	47.815%
0.004	303.879	3.879	64.890	53.015%
0.005	303.472	3.472	72.603	59.316%

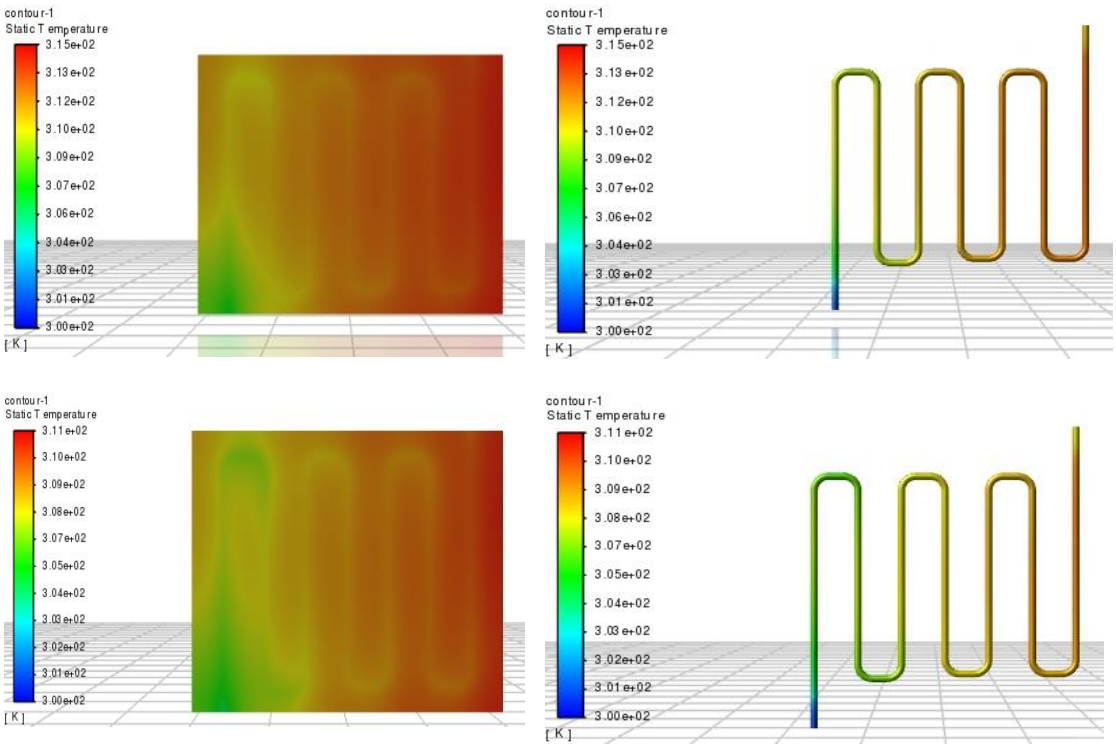

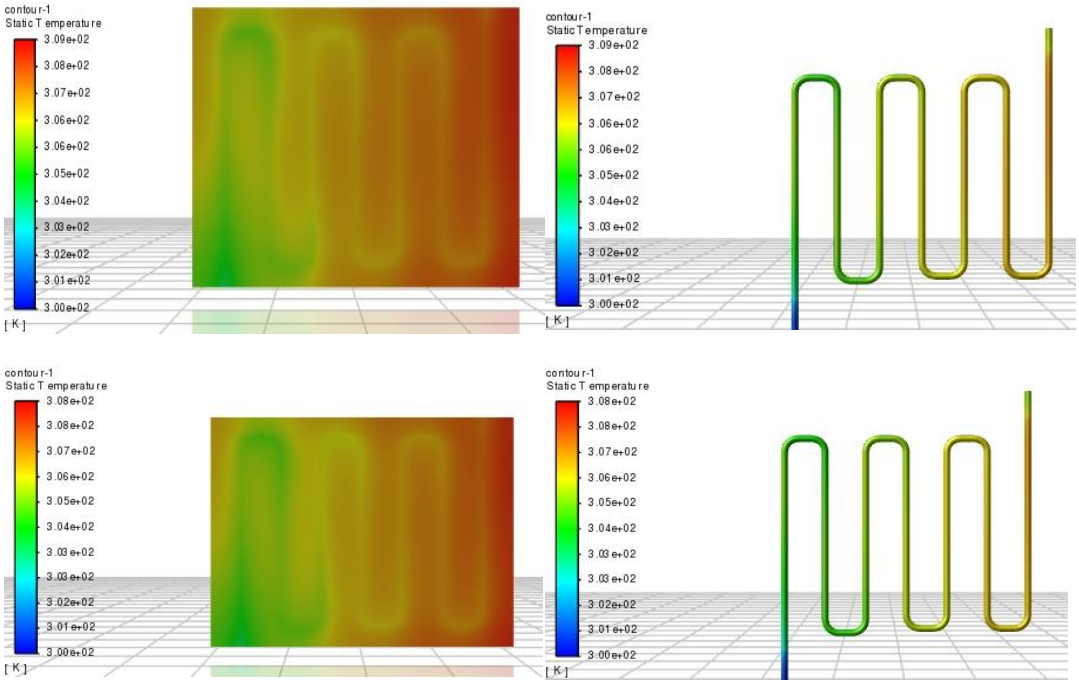

Temperature contour of PV panel and pipes for 0.001 to 0.004 kg/sec at 800 W/m^2 in sequential order

Thermal efficiency at 1000 W/m^2 for various mass flow rate

ṁ (kg/sec)	T_{out} (K)	ΔT (K)	Qu (Watt)	η_{th} (%)
0.001	311.823	11.823	49.442	32.315%
0.002	307.614	7.614	63.683	41.623%
0.003	305.832	5.832	73.169	47.823%
0.004	304.850	4.850	81.130	53.026%
0.005	304.341	4.341	90.775	59.330%

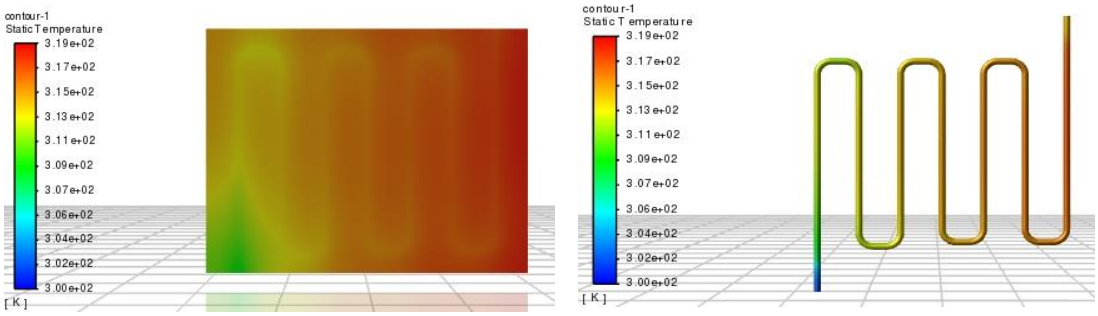

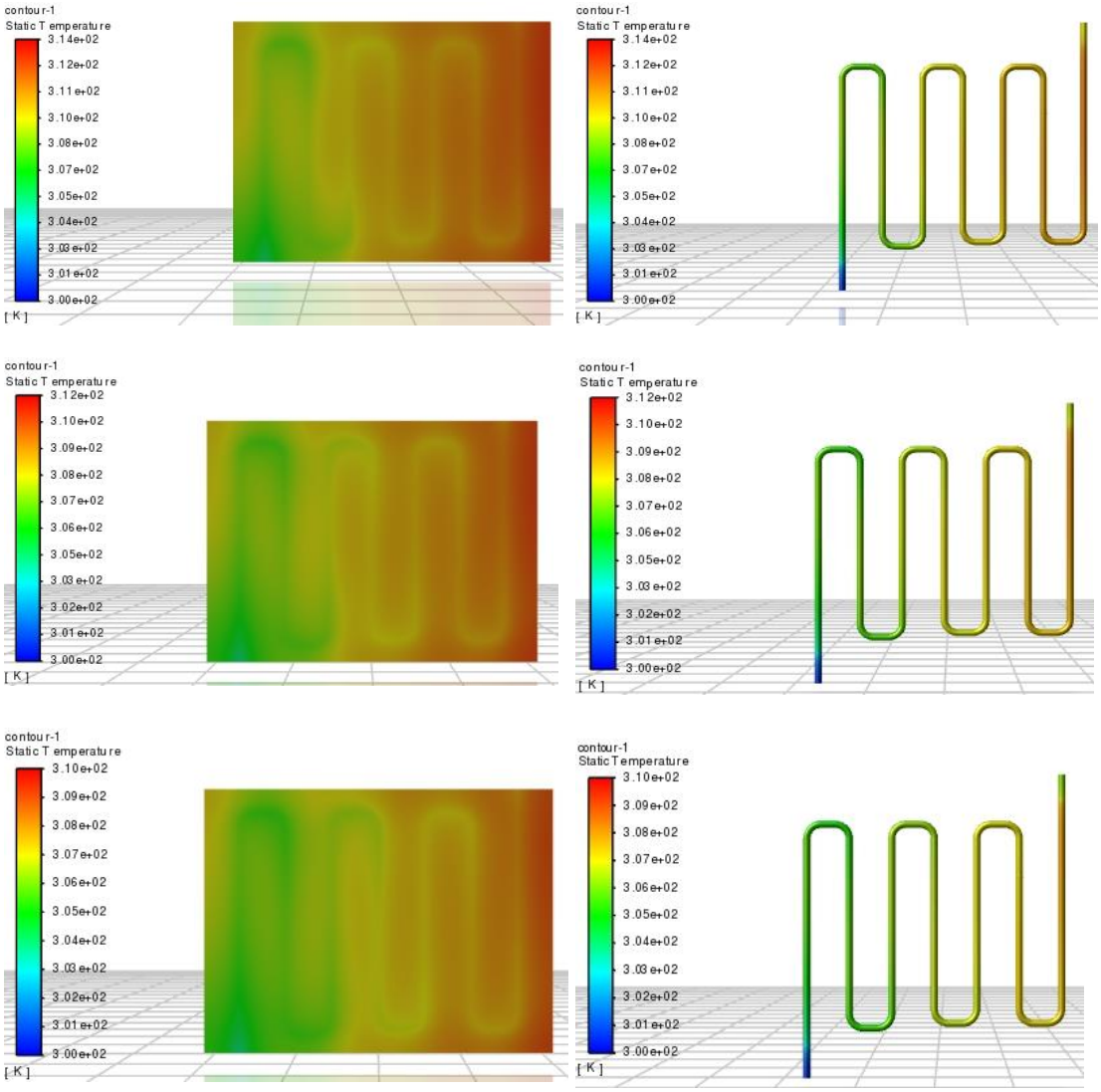

Temperature contour of PV panel and pipes for 0.001 to 0.004 kg/sec at 1000 W/m^2 in sequential order

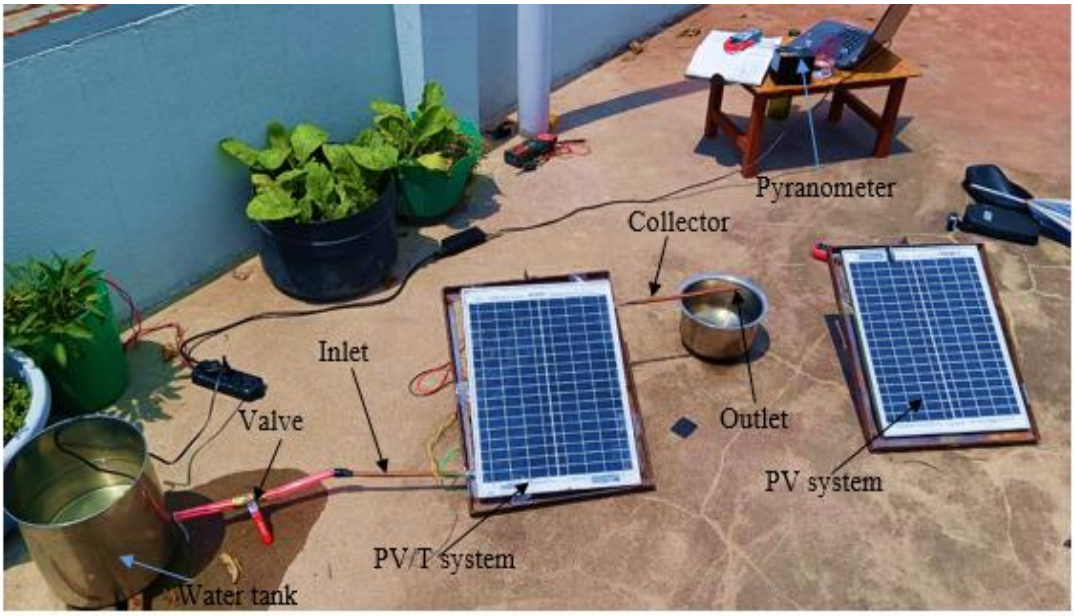

Experimental setup

Temperature measurement

Thermal absorber and collector

Table: Experimental Data

25/4/2080						
Flow (kg/sec)		0.001	0.002	0.0033	0.004	0.005
Inlet temp.(K)		297	298.5	300	302	303
Outlet temp. (K)		306	304.5	304	305.5	306.5
Temp. diff. (K)		9	6	4	3.5	3.5
For PVT	Voltage (V)	19.96	19.9	19.89	19.74	19.69
	Current (A)	0.57	0.62	0.66	0.66	0.71
For PV	Voltage (V)	20.1	19.95	19.63	19.79	19.98
	Current (A)	0.52	0.57	0.61	0.6	0.64
PV cell temp. (K)		314	314	313	312	310
PVT cell temp. (K)		311	309	309	306	305
Irradiance (W/m^2)		820	840	860	800	860
PVT	η_{th}	30.00%	39.05%	41.95%	47.83%	55.62%
	η_{ele}	9.07%	9.60%	9.98%	10.64%	10.62%
	η_o	39.07%	48.65%	51.93%	58.48%	66.24%
PV	η_{ele}	8.33%	8.85%	9.10%	9.70%	9.72%
Power (watt)	PV	10.45	11.37	11.97	11.87	12.79
	PVT	11.38	12.34	13.13	13.03	13.98
26/4/2080						
Flow (kg/sec)		0.001	0.002	0.0033	0.004	0.005
Inlet temp.(K)		299.5	300.5	301	302.5	304
Outlet temp. (K)		308.5	306.5	305	306	307.5
Temp. diff. (K)		9	6	4	3.5	3.5
For PVT	Voltage (V)	20	19.92	19.88	19.81	19.65
	Current (A)	0.59	0.66	0.66	0.68	0.71
For PV	Voltage (V)	20.1	19.81	19.63	19.79	19.75
	Current (A)	0.54	0.61	0.62	0.62	0.64
PV cell temp. (K)		315	315	313	312	310
PVT cell temp. (K)		311	309	309	306	305
Irradiance (W/m^2)		840	860	840	820	860
PVT	η_{th}	29.29%	38.14%	42.95%	46.67%	55.62%
	η_{ele}	9.18%	9.99%	10.21%	10.74%	10.60%
	η_o	38.47%	48.13%	53.16%	57.40%	66.22%
PV	η_{ele}	8.45%	9.18%	9.47%	9.78%	9.61%
Power (watt)	PV	10.85	12.08	12.17	12.27	12.64
	PVT	11.80	13.15	13.12	13.47	13.95

27/4/2080						
Flow (kg/sec)		0.001	0.002	0.0033	0.004	0.005
Inlet temp.(K)		299.5	300.5	301	303	304
Outlet temp. (K)		308	306.5	305	306.5	307.5
Temp. diff. (K)		8.5	6	4	3.5	3.5
For PVT	Voltage (V)	20	19.96	19.89	19.92	19.78
	Current (A)	0.55	0.65	0.65	0.7	0.71
For PV	Voltage (V)	20.1	19.86	19.63	19.79	19.75
	Current (A)	0.5	0.6	0.62	0.66	0.67
PV cell temp. (K)		315	315	313	312	310
PVT cell temp. (K)		311	309	309	306	305
Irradiance (W/m^2)		820	860	820	820	860
PVT	η_{th}	28.33%	38.14%	44.00%	46.67%	55.62%
	η_{ele}	8.77%	9.86%	10.30%	11.11%	10.67%
	η_o	37.10%	48.00%	54.30%	57.78%	66.29%
PV	η_{ele}	8.01%	9.06%	9.70%	10.41%	10.06%
Power (watt)	PV	10.05	11.92	12.17	13.06	13.23
	PVT	11.00	12.97	12.93	13.94	14.04

32/4/2080						
Flow (kg/sec)		0.001	0.002	0.0033	0.004	0.005
Inlet temp.(K)		301	303.5	304.5	305.5	306
Outlet temp. (K)		309	309	308.5	309	309
Temp. diff. (K)		8	5.5	4	3.5	3
For PVT	Voltage (V)	20	19.9	19.89	19.92	19.78
	Current (A)	0.51	0.55	0.59	0.63	0.63
For PV	Voltage (V)	19.94	19.83	19.79	19.87	19.71
	Current (A)	0.48	0.52	0.55	0.58	0.6
PV cell temp. (K)		310	310	312	312	310
PVT cell temp. (K)		308	307	309	308	307
Irradiance (W/m^2)		780	820	840	840	800
PVT	η_{th}	28.03%	36.67%	42.95%	45.56%	51.25%
	η_{ele}	8.55%	8.72%	9.13%	9.76%	10.18%
	η_o	36.58%	45.39%	52.08%	55.32%	61.43%
PV	η_{ele}	8.02%	8.22%	8.47%	8.97%	9.66%
Power (watt)	PV	9.57	10.31	10.88	11.52	11.83
	PVT	10.20	10.95	11.74	12.55	12.46

1/5/2080						
Flow (kg/sec)		0.001	0.002	0.0033	0.004	0.005
Inlet temp.(K)		302	303	305	308	307
Outlet temp. (K)		311	308.5	309	311.5	310.5
Temp. diff.(K)		9	5.5	4	3.5	3.5
For PVT	Voltage (V)	19.78	19.74	19.6	19.95	19.8
	Current (A)	0.56	0.59	0.65	0.69	0.69
For PV	Voltage (V)	19.8	19.9	19.8	20	20.1
	Current (A)	0.52	0.55	0.6	0.64	0.64
PV cell temp. (K)		316	308	313	318	318
PVT cell temp. (K)		313	306	309	313	313
Irradiance (W/m^2)		820	780	820	800	860
PVT	η_{th}	30.00%	38.55%	44.00%	47.83%	55.62%
	η_{ele}	8.83%	9.76%	10.15%	11.25%	10.38%
	η_o	38.83%	48.31%	54.15%	59.08%	66.00%
PV	η_{ele}	8.21%	9.17%	9.47%	10.46%	9.78%
Power (watt)	PV	10.30	10.95	11.88	12.80	12.86
	PVT	11.08	11.65	12.74	13.77	13.66

2/5/2080						
Flow (kg/sec)		0.001	0.002	0.0033	0.004	0.005
Inlet temp.(K)		294	296	299	302	304
Outlet temp. (K)		302	302	303	305.5	307
Temp. diff. (K)		8	6	4	3.5	3
For PVT	Voltage (V)	20.5	19.75	19.61	19.81	19.98
	Current (A)	0.52	0.6	0.65	0.65	0.67
For PV	Voltage (V)	20.4	19.7	19.55	19.78	19.91
	Current (A)	0.48	0.55	0.58	0.59	0.6
PV cell temp. (K)		304	305	312	310	308
PVT cell temp. (K)		302	303	309	308	306
Irradiance (W/m^2)		820	860	860	840	820
PVT	η_{th}	26.67%	38.14%	41.95%	45.56%	50.00%
	η_{ele}	8.50%	9.01%	9.69%	10.02%	10.67%
	η_o	35.16%	47.15%	51.64%	55.57%	60.67%
PV	η_{ele}	7.80%	8.23%	8.62%	9.08%	9.52%
Power (watt)	PV	9.79	10.84	11.34	11.67	11.95
	PVT	10.66	11.85	12.75	12.88	13.39

3/5/2080						
Flow (kg/sec)		0.001	0.002	0.0033	0.004	0.005
Inlet temp.(K)		301	302	303	303.5	305
Outlet temp. (K)		309	308	306.5	307	308
Temp. diff (K)		8	6	3.5	3.5	3
For PVT	Voltage (V)	19.8	19.9	20.4	20	19.5
	Current (A)	0.53	0.59	0.59	0.62	0.62
For PV	Voltage (V)	19.75	19.85	20.25	19.95	19.45
	Current (A)	0.5	0.54	0.58	0.6	0.6
PV cell temp. (K)		310	309	310	313	314
PVT cell temp. (K)		307	307	308	311	311
Irradiance (W/m^2)		800	840	820	840	800
PVT	η_{th}	27.33%	39.05%	38.50%	45.56%	51.25%
	η_{ele}	8.57%	9.14%	9.59%	9.65%	9.88%
	η_o	35.91%	48.18%	48.09%	55.20%	61.13%
PV	η_{ele}	8.07%	8.34%	9.36%	9.31%	9.53%
Power (watt)	PV	9.88	10.72	11.75	11.97	11.67
	PVT	10.49	11.74	12.04	12.40	12.09
Average of 7 days						
Flow (kg/sec)		0.001	0.002	0.0033	0.004	0.005
Inlet temp.(K)		299.143	300.571	301.929	303.786	304.714
Outlet temp. (K)		307.643	306.429	305.857	307.286	308.000
Temp. diff(K)		8.500	5.857	3.929	3.500	3.286
For PVT	Voltage (V)	20.006	19.867	19.880	19.879	19.740
	Current (A)	0.547	0.609	0.636	0.661	0.677
For PV	Voltage (V)	20.027	19.843	19.754	19.853	19.807
	Current (A)	0.506	0.563	0.594	0.613	0.627
PV cell temp. (K)		312.00	310.86	312.29	312.71	311.43
PVT cell temp. (K)		309.00	307.14	308.86	308.29	307.43
Irradiance (W/m2)		814.29	837.14	837.14	822.86	837.14
PVT	η_{th}	28.52%	38.25%	42.33%	46.52%	53.57%
	η_{ele}	8.78%	9.44%	9.87%	10.45%	10.43%
	η_o	37.30%	47.69%	52.20%	56.98%	64.00%
PV	η_{ele}	8.13%	8.72%	9.17%	9.67%	9.70%
Power (watt)	PV	10.13	11.17	11.74	12.17	12.42
	PVT	10.94	12.09	12.63	13.15	13.17

त्रिभुवन विश्वविद्यालय
Tribhuvan University
इन्जिनियरिङ अध्ययन संस्थान
Institute of Engineering
डीनको कार्यालय
OFFICE OF THE DEAN

GPO box- 1915, Pulchowk, Lalitpur
Tel: 977-5-521531, Fax: 977-5-525830
dean@ioe.edu.np, www.ioe.edu.np
गोश्वारा पो ब न- १९१५, पुल्चोक, ललितपुर
फोन- ५५२१५३१, फ्याक्स- ५५२५८३०

Date: November 26, 2023

To Whom It May Concern:

This is to certify that the paper titled "***Analysis of solar photovoltaic-thermal system using an experimental and simulation approach***" (Submission# **373**) submitted by **Ashok Subedi** as the first author has been accepted after the peer-review process for presentation in the 14th IOE Graduate Conference being held during Nov 29 to Dec 1, 2023. Kindly note that the publication of the conference proceedings is still underway and hence inclusion of the accepted manuscript in the conference proceedings is contingent upon the author's presence for presentation during the conference and timely response to further edits during the publication process.

Bhim Kumar Dahal, PhD
Convener,
14th IOE Graduate Conference

Analysis of Solar Photovoltaic-Thermal System Using Simulation and Experimental Approach

ORIGINALITY REPORT

7%
SIMILARITY INDEX

PRIMARY SOURCES

1	Husam Abdulrasool Hasan, Kamaruzzaman Sopian, Ahed Hameed Jaaz, Ali Najah Al-Shamani. "Experimental investigation of jet array nanofluids impingement in photovoltaic/thermal collector", Solar Energy, 2017 Crossref	73 words — < 1%
2	Imtiaz Ali Laghari, Mahendran Samykano, Adarsh Kumar Pandey, Kumaran Kadirgama, Vineet Veer Tyagi. "Advancements in PV-Thermal Systems with and without Phase Change Materials as Sustainable Energy Solution: Energy, Exergy and Exergoeconomic (3E) Analysis approach", Sustainable Energy & Fuels, 2020 Crossref	58 words — < 1%
3	academic.oup.com Internet	58 words — < 1%
4	wecs.gov.np Internet	58 words — < 1%
5	ir.knust.edu.gh Internet	38 words — < 1%
6	Awaneendra Kumar Tiwari, Kalyan Chatterjee, Vinay Kumar Deolia. "Application of Copper Oxide	28 words — < 1%

Nanofluid and Phase Change Material on the Performance of Hybrid Photovoltaic–Thermal (PVT) System", Processes, 2023
Crossref

7	A.M. Elbreki, M.A. Alghoul, A.N. Al-Shamani, A.A. Ammar, Bita Yegani, Alsanossi M. Aboghrara, M.H. Rusaln, K. Sopian. "The role of climatic-design-operational parameters on combined PV/T collector performance: A critical review", Renewable and Sustainable Energy Reviews, 2016 Crossref	27 words —	< 1%
8	hdl.handle.net Internet	26 words —	< 1%
9	Zahra Zareie, Rouhollah Ahmadi, Mahdi Asadi. "A comprehensive numerical investigation of a branch-inspired channel in roll-bond type PVT system using design of experiments approach", Energy, 2023 Crossref	25 words —	< 1%
10	digiresearch.vut.ac.za Internet	25 words —	< 1%
11	Arman Kolahan, Seyed Reza Maadi, Arash Kazemian, Corrado Schenone, Tao Ma. "Semi-3D transient simulation of a nanofluid-base photovoltaic thermal system integrated with a thermoelectric generator", Energy Conversion and Management, 2020 Crossref	22 words —	< 1%
12	core.ac.uk Internet	20 words —	< 1%
13	vdoc.pub Internet	20 words —	< 1%

14	Feng Shan, Fang Tang, Lei Cao, Guiyin Fang. "Performance evaluations and applications of photovoltaic–thermal collectors and systems", Renewable and Sustainable Energy Reviews, 2014 Crossref	19 words — < 1%
15	Gökhan Yıldız, Ali Etem Gürel, İlhan Ceylan, Alper Ergün, Mehmet Onur Karaağaç, Ümit Ağbulut. "Thermodynamic analyses of a novel hybrid photovoltaic-thermal (PV/T) module assisted vapor compression refrigeration system", Journal of Building Engineering, 2023 Crossref	19 words — < 1%
16	Madalina Barbu, George Darie, Monica Siroux. "A Parametric Study of a Hybrid Photovoltaic Thermal (PVT) System Coupled with a Domestic Hot Water (DHW) Storage Tank", Energies, 2020 Crossref	19 words — < 1%
17	www.mdpi.com Internet	18 words — < 1%
18	www.in-car-stuff.com Internet	17 words — < 1%
19	Dubey, S.. "Analytical expression for electrical efficiency of PV/T hybrid air collector", Applied Energy, 200905 Crossref	15 words — < 1%
20	J.F. Chen, L. Zhang, Y.J. Dai. "Performance analysis and multi-objective optimization of a hybrid photovoltaic/thermal collector for domestic hot water application", Energy, 2018 Crossref	13 words — < 1%

21	ROONAK DAGHIGH, MOHD HAFIDZ RUSLAN, KAMARUZZAMAN SOPIAN. "Parametric studies of an active solar water heating system with various types of PVT collectors", Sadhana, 2015 Crossref	13 words — < 1%
22	Rohan S. Kulkarni, Rajani B. Shinde, Dhananjay B. Talange. "Performance Evaluation and a New Thermal Model for a Photovoltaic-Thermal Water Collector System", 2018 International Conference on Smart Grid and Clean Energy Technologies (ICSGCE), 2018 Crossref	13 words — < 1%
23	ulster.pure.elsevier.com Internet	13 words — < 1%
24	upcommons.upc.edu Internet	13 words — < 1%
25	www.ros.hw.ac.uk Internet	13 words — < 1%
26	Yuan, Han, Ning Mei, and Peilin Zhou. "Performance analysis of an absorption power cycle for ocean thermal energy conversion", Energy Conversion and Management, 2014. Crossref	12 words — < 1%
27	repository.up.ac.za Internet	12 words — < 1%
28	Amarnath, H. K.. "An investigation on the performance of a direct injection diesel engine using esterified oils (biodiesels) as fuel.", Proquest, 2016. ProQuest	11 words — < 1%

29	Lertsatitthanakorn, C.. "Performance analysis of a double-pass thermoelectric solar air collector", Solar Energy Materials and Solar Cells, 200809 Crossref	11 words — < 1%
30	Niusha Hooshmandzade, Ali Motevali, Seyed Reza Mousavi Seyedi, Pouria Biparva. "Influence of single and hybrid water-based nanofluids on performance of microgrid photovoltaic/thermal system", Applied Energy, 2021 Crossref	11 words — < 1%
31	Pondyal, Khem N, Binod K Bhattarai, Balkrishna Sapkota, and Berit Kjeldstad. "Solar Radiation Potential at Four Sites of Nepal", Journal of the Institute of Engineering, 2012. Crossref	11 words — < 1%
32	www.flowmerics.com Internet	11 words — < 1%
33	Banerjee, Ishita. "Determination of Lubricant Quality Using Maximum Bubble Pressure Method", Auburn University, 2023 ProQuest	10 words — < 1%
34	Jain, Aakrati. "Characterization of Flow Freezing in Small Channels for Ice Valve Applications", Purdue University, 2023 ProQuest	10 words — < 1%
35	S. V. Vimal, S. S. Surya. "Performance Analysis of Solar Water Heater with Various Working Fluids", Journal of Mines, Metals and Fuels, 2022 Crossref	10 words — < 1%
36	Yuji Nakamura, Shota Endo. "Power generation performance of direct flame fuel cell (DFFC)	10 words — < 1%

impinged by small jet flames", Journal of Micromechanics and Microengineering, 2015
Crossref

37 dspace.mit.edu
Internet
10 words — < 1%

38 repository.upi.edu
Internet
10 words — < 1%

39 umpir.ump.edu.my
Internet
10 words — < 1%

40 www.oaklease.co.uk
Internet
10 words — < 1%

41 "Fundamental and Applied Scientific Research in the Development of Agriculture in the Far East (AFE-2022)", Springer Science and Business Media LLC, 2023
Crossref
9 words — < 1%

42 Amirhossian Chaysaz, Seyed Reza Mousavi Seyedi, Ali Motevali. "Effects of different greenhouse coverings on energy parameters of a photovoltaic–thermal solar system", Solar Energy, 2019
Crossref
9 words — < 1%

43 Bondoc, Christopher Carl Eduardo. "Feasibility and Environmental Life Cycle Assessment of Mono-Crystalline Silicon (Mono-Si) Solar Photovoltaic Panels with Recycled Vs. Non-Recycled Materials", Villanova University, 2023
ProQuest
9 words — < 1%

44 Joshi, A.S.. "Performance evaluation of a hybrid photovoltaic thermal (PV/T) (glass-to-glass) system", International Journal of Thermal Sciences, 200901
Crossref
9 words — < 1%

45 Li, X., Y.J. Dai, Y. Li, and R.Z. Wang. "Comparative study on two novel intermediate temperature CPC solar collectors with the U-shape evacuated tubular absorber", Solar Energy, 2013. 9 words — < 1%
Crossref

46 Milad Teymori-omran, Ali Motevali, Seyed Reza Mousavi Seyedi, Mehdi Montazeri. "Numerical simulation and experimental validation of a photovoltaic/thermal system: Performance comparison inside and outside greenhouse", Sustainable Energy Technologies and Assessments, 2021 9 words — < 1%
Crossref

47 Mohan, Sujith, and S. O. Bade Shrestha. "Evaluation of the Performance Characteristics of a Direct Methanol Fuel Cell With Multi Fuels", ASME 2009 7th International Conference on Fuel Cell Science Engineering and Technology, 2009. 9 words — < 1%
Crossref

48 Mostapha Oulcaid, Hassan El Fadil, Leila Ammeh, Abdelhafid Yahya, Fouad Giri. "One shape parameter-based explicit model for photovoltaic cell and panel", Sustainable Energy, Grids and Networks, 2020 9 words — < 1%
Crossref

49 Prakash M. Shrestha, Khem N Poudyal, Narayan P. Chapagain, Indra B. Karki. "Study of Impact of Linke Turbidity on Solar Radiation over Kathmandu Valley", Patan Pragya, 2020 9 words — < 1%
Crossref

50 S. Christopher, V. Kumaresan, K.S. Raghavan. "Role of thermal energy storage for enhancing thermal performance of evacuated tube with compound parabolic 9 words — < 1%

concentrator collector", International Journal of Energy Research, 2020
Crossref

51 Solanki, S.C.. "Indoor simulation and testing of photovoltaic thermal (PV/T) air collectors", Applied Energy, 200911 — 9 words — < 1%
Crossref

52 Weitao Liu, Xunda Zhang, Cuishuang Guo, Dengxin Ai, Baoquan Yin. "Performance research of the PVT-coupled water loop heat pump system", Journal of Physics: Conference Series, 2023 — 9 words — < 1%
Crossref

53 Xin Tang, Guiqiang Li, Xudong Zhao. "Performance analysis of a novel hybrid electrical generation system using photovoltaic/thermal and thermally regenerative electrochemical cycle", Energy, 2021 — 9 words — < 1%
Crossref

54 Xinyue Han, Fan Ding, Ju Huang, Xiaobo Zhaoa. "Hybrid nanofluid filtered concentrating photovoltaic/thermal-direct contact membrane distillation system for co-production of electricity and freshwater", Energy, 2022 — 9 words — < 1%
Crossref

55 Zhonghe Han, Kaixin Liu, Guiqiang Li, Xudong Zhao, Samson Shittu. "Electrical and thermal performance comparison between PVT-ST and PV-ST systems", Energy, 2021 — 9 words — < 1%
Crossref

56 etd.auburn.edu — 9 words — < 1%
Internet

57 ir-library.egerton.ac.ke

	Internet	9 words — < 1%
58	ir.library.ui.edu.ng Internet	9 words — < 1%
59	theses.lib.polyu.edu.hk Internet	9 words — < 1%
60	www.diva-portal.org Internet	9 words — < 1%

EXCLUDE QUOTES	ON	EXCLUDE SOURCES	< 6 WORDS
EXCLUDE BIBLIOGRAPHY	ON	EXCLUDE MATCHES	< 9 WORDS